with p37 and p42 fragments, and additionally, p37 in native GAMA might *per se* mediate interaction with a different receptor that is neuraminidase and chymotrypsin resistant. Identification of the GAMA receptor(s) in future studies will be important to understanding the binding specificities of GAMA. Taken together, these results indicate that GAMA binds a nonsialylated protein receptor, and hence, GAMA represents a novel SA-independent invasion ligand that plays a role in the SA-independent invasion pathway. Our results indicating that the invasion-inhibitory effect of anti-FL is more profound with neuraminidase-treated erythrocytes (i.e., 72%; Fig. 4B) than with untreated erythrocytes (i.e., 38%; Fig. 4A) validate that GAMA indeed plays a role in the SA-independent invasion pathway.

Invasion pathways can be broadly classified into 2 main groups based on the use of SA on the erythrocyte surface by parasite ligands (22): (i) SA-independent (neuraminidase-resistant) invasion (11, 31) and (ii) SA-dependent (neuraminidase-sensitive) invasion (5, 17, 23, 26). Therefore, we were interested in finding combinations of antigens that induce more-potent synergistic antiparasite activity. Our results (Fig. 6) indicating that a combination of antibodies against GAMA (an SA-independent ligand) and EBA175 (an SA-dependent ligand) exhibited a significantly greater invasion-inhibitory effect than either anti-GAMA or anti-EBA175 antibody alone support the rationale that, for achieving greater invasion inhibition, targeting of both SA-dependent and SA-independent ligands/pathways is better than targeting either of them alone. It will be worthwhile to further test whether a more potent, or possibly synergistic, antiparasitic activity can be achieved with either a combination vaccine (mixture of GAMA and EBA175 antigens) or a fusion vaccine (chimeric GAMA-EBA175 fusion protein) *in vivo*.

Based on the colocalization of GAMA and AMA1 (Fig. 3A), we also hypothesized that the combination of anti-GAMA and anti-AMA1 antibodies might exhibit a greater invasion-inhibitory effect than either of them alone. However, our results (Fig. 6) showed that it was not the case. Given that GAMA interacts with an unknown erythrocyte receptor and AMA1 interacts with RON2 (30), one of the plausible explanations for our result is that GAMA-erythrocyte receptor interaction might be upstream of the AMA1-RON2 interaction and blocking of GAMA-receptor interaction by anti-GAMA antibodies makes the downstream AMA1-RON2 interaction impossible and, hence, renders the inhibitory effect of anti-AMA1 antibody superfluous.

Immunoreactive antigens involved in erythrocyte invasion represent potential candidates for malaria vaccine development (10), and designing a vaccine based on sequences of immunoreactive antigens with minimum polymorphisms is critical to preventing the parasite from evading the vaccine-induced immunity. Our results indicating that GAMA is localized on the surface of free merozoite (Fig. 3A) and antibodies are generated against GAMA during natural infection in humans (Fig. 7) suggest that GAMA is an immunogenic antigen. In order to study whether GAMA is exposed to the host immune pressure, we compared the single nucleotide polymorphisms (SNPs) in GAMA of 12 laboratory strains (see Table S1 in the supplemental material) deposited in PlasmoDB (http://plasmodb.org/plasmo/). GAMA contains a total of 7 nonsynonymous SNPs, and importantly, there are only 4 nonsynonymous SNPs outside the long asparagine-rich region (residues 356 to 485 in Fig. 1A); 3 of them (at positions 67, 229, and 258) are in Tr1, and only 1 (at position 632) is in the Tr3 region (containing the erythrocyte binding epitope) of GAMA. These preliminary SNP analyses suggest that GAMA is less polymorphic and, hence, may be a promising blood-stage vaccine candidate antigen. However, to validate this claim, we need further analysis of SNPs of GAMA in different field isolates worldwide.

In contrast to peripheral merozoite surface proteins and other apical proteins, most GPI-anchored proteins are refractory to genetic deletion (28). Knockouts of the GAMA gene in 3D7 and W2mef strains of *P. falciparum* were attempted, but no GAMA gene deletion mutant could be generated (see Fig. S1 in the supplemental material), and thus we believe that GAMA is essential to *P. falciparum* parasite invasion. However, it can be seen that the genetic disruption of the GAMA ortholog was successful in *P. berghei* (12). This discrepancy may be due to the differences in host erythrocyte receptors. However, additional research is required to address this discrepancy.

In summary, our data establish that GAMA is an important micronemal antigen. The data indicating that GAMA is exposed to the human immune system and anti-GAMA antibodies block merozoite invasion of erythrocytes *in vitro* validate GAMA as a novel blood-stage vaccine candidate antigen and suggest that it may be a target of antibodies that contribute to acquired immunity to malaria. Erythrocyte binding assays revealed that GAMA possesses an erythrocyte binding epitope in the C-terminal region and it binds a nonsialylated protein receptor. Growth inhibition assays with neuraminidase-treated erythrocytes reveal that GAMA represents a ligand that plays a role in the SA-independent invasion pathway. The significantly greater invasion-inhibitory effect exhibited by the combination of anti-GAMA or anti-EBA175 antibodies supports the rationale that targeting of both SA-dependent and SA-independent ligands/pathways is better than targeting either of them alone. This study also substantiates that the wheat germ cell-free system is a valuable tool for identification of novel malaria vaccine candidates.

ACKNOWLEDGMENTS

We thank Masachika Shudo, Integrated Center for Science, Ehime University, Japan, for technical assistance. We also thank the Japanese Red Cross Society for providing us the human erythrocytes and human plasma.

This research was supported in part by grants from The Bill and Melinda Gates Foundation, from the Ministry of Education, Culture, Sports, Science and Technology (21249028, 21022034, 23406007, and 23117008), and from the Ministry of Health, Labor, and Welfare, Japan (H21-Chikyukibo-ippan-005). This study was supported in part by the intramural program of the National Institute of Allergy and Infectious Diseases/NIH, and the GIA Reference Center is supported by the PATH/Malaria Vaccine Initiative.

REFERENCES

1. **Abramoff, M. D., P. J. Magalhaes, and S. J. Ram.** 2004. Image processing with ImageJ. Biophotonics Int. **11**:36–42.
2. **Bei, A. K., et al.** 2010. A flow cytometry-based assay for measuring invasion of red blood cells by *Plasmodium falciparum*. Am. J. Hematol. **85**:234–237.
3. **Birkett, A. J.** 2010. PATH Malaria Vaccine Initiative (MVI): perspectives on the status of malaria vaccine development. Hum. Vaccin. **6**:139–145.

4. **Bozdech, Z., et al.** 2003. The transcriptome of the intraerythrocytic developmental cycle of *Plasmodium falciparum*. PLoS Biol. **1**:E5.
5. **Camus, D., and T. J. Hadley.** 1985. A *Plasmodium falciparum* antigen that binds to host erythrocytes and merozoites. Science **230**:553–556.
6. **Cao, J., et al.** 2009. Rhoptry neck protein RON2 forms a complex with microneme protein AMA1 in *Plasmodium falciparum* merozoites. Parasitol. Int. **58**:29–35.
7. **Coleman, R. E., et al.** 2004. Infectivity of asymptomatic *Plasmodium*-infected human populations to Anopheles dirus mosquitoes in western Thailand. J. Med. Entomol. **41**:201–208.
8. **Crompton, P. D., et al.** 2010. In vitro growth-inhibitory activity and malaria risk in a cohort study in Mali. Infect. Immun. **78**:737–745.
9. **Deans, A. M., et al.** 2007. Invasion pathways and malaria severity in Kenyan *Plasmodium falciparum* clinical isolates. Infect. Immun. **75**:3014–3020.
10. **Doolan, D. L., et al.** 2008. Profiling humoral immune responses to *P. falciparum* infection with protein microarrays. Proteomics **8**:4680–4694.
11. **Duraisingh, M. T., et al.** 2003. Phenotypic variation of *Plasmodium falciparum* merozoite proteins directs receptor targeting for invasion of human erythrocytes. EMBO J. **22**:1047–1057.
12. **Ecker, A., E. S. Bushell, R. Tewari, and R. E. Sinden.** 2008. Reverse genetics screen identifies six proteins important for malaria development in the mosquito. Mol. Microbiol. **70**:209–220.
13. **Florens, L., et al.** 2002. A proteomic view of the *Plasmodium falciparum* life cycle. Nature **419**:520–526.
14. **Fowkes, F. J., J. S. Richards, J. A. Simpson, and J. G. Beeson.** 2010. The relationship between anti-merozoite antibodies and incidence of *Plasmodium falciparum* malaria: a systematic review and meta-analysis. PLoS Med. **7**:e1000218.
15. **Gardner, M. J., et al.** 2002. Genome sequence of the human malaria parasite *Plasmodium falciparum*. Nature **419**:498–511.
16. **Genton, B.** 2008. Malaria vaccines: a toy for travelers or a tool for eradication? Expert Rev. Vaccines **7**:597–611.
17. **Gilberger, T. W., et al.** 2003. A novel erythrocyte binding antigen-175 paralogue from *Plasmodium falciparum* defines a new trypsin-resistant receptor on human erythrocytes. J. Biol. Chem. **278**:14480–14486.
18. **Gilson, P. R., et al.** 2006. Identification and stoichiometry of glycosylphosphatidylinositol-anchored membrane proteins of the human malaria parasite *Plasmodium falciparum*. Mol. Cell Proteomics **5**:1286–1299.
19. **Greenwood, B. M., et al.** 2008. Malaria: progress, perils, and prospects for eradication. J. Clin. Invest. **118**:1266–1276.
20. **Haase, S., et al.** 2008. Characterization of a conserved rhoptry-associated leucine zipper-like protein in the malaria parasite *Plasmodium falciparum*. Infect. Immun. **76**:879–887.
21. **Hinds, L., J. L. Green, E. Knuepfer, M. Grainger, and A. A. Holder.** 2009. Novel putative glycosylphosphatidylinositol-anchored micronemal antigen of *Plasmodium falciparum* that binds to erythrocytes. Eukaryot. Cell **8**:1869–1879.
22. **Lopaticki, S., et al.** 2011. Reticulocyte and erythrocyte binding-like proteins function cooperatively in invasion of human erythrocytes by malaria parasites. Infect. Immun. **79**:1107–1117.
23. **Maier, A. G., et al.** 2003. *Plasmodium falciparum* erythrocyte invasion through glycophorin C and selection for Gerbich negativity in human populations. Nat. Med. **9**:87–92.
24. **McCallum, F. J., et al.** 2008. Acquisition of growth-inhibitory antibodies against blood-stage *Plasmodium falciparum*. PLoS One **3**:e3571.
25. **Persson, K. E., C. T. Lee, K. Marsh, and J. G. Beeson.** 2006. Development and optimization of high-throughput methods to measure *Plasmodium falciparum*-specific growth inhibitory antibodies. J. Clin. Microbiol. **44**:1665–1673.
26. **Persson, K. E., et al.** 2008. Variation in use of erythrocyte invasion pathways by *Plasmodium falciparum* mediates evasion of human inhibitory antibodies. J. Clin. Invest. **118**:342–351.
27. **Richards, J. S., and J. G. Beeson.** 2009. The future for blood-stage vaccines against malaria. Immunol. Cell Biol. **87**:377–390.
28. **Sanders, P. R., et al.** 2006. A set of glycosylphosphatidyl inositol-anchored membrane proteins of *Plasmodium falciparum* is refractory to genetic deletion. Infect. Immun. **74**:4330–4338.
29. **Singh, K., et al.** 2010. Subdomain 3 of *Plasmodium falciparum* VAR2CSA DBL3x is identified as a minimal chondroitin sulfate A-binding region. J. Biol. Chem. **285**:24855–24862.
30. **Srinivasan, P., et al.** 2011. Binding of *Plasmodium* merozoite proteins RON2 and AMA1 triggers commitment to invasion. Proc. Natl. Acad. Sci. U. S. A. **108**:13275–13280.
31. **Stubbs, J., et al.** 2005. Molecular mechanism for switching of *P. falciparum* invasion pathways into human erythrocytes. Science **309**:1384–1387.
32. **Takeo, S., T. U. Arumugam, M. Torii, and T. Tsuboi.** 2009. Wheat germ cell-free technology for accelerating the malaria vaccine research. Expert Opin. Drug Discov. **4**:1191–1199.
33. **Tham, W. H., et al.** 2010. Complement receptor 1 is the host erythrocyte receptor for *Plasmodium falciparum* PfRh4 invasion ligand. Proc. Natl. Acad. Sci. U. S. A. **107**:17327–17332.
34. **Tsuboi, T., S. Takeo, T. U. Arumugam, H. Otsuki, and M. Torii.** 2010. The wheat germ cell-free protein synthesis system: a key tool for novel malaria vaccine candidate discovery. Acta Trop. **114**:171–176.
35. **Tsuboi, T., et al.** 2008. Wheat germ cell-free system-based production of malaria proteins for discovery of novel vaccine candidates. Infect. Immun. **76**:1702–1708.
36. **Tsuboi, T., S. Takeo, T. Sawasaki, M. Torii, and Y. Endo.** 2010. An efficient approach to the production of vaccines against the malaria parasite. Methods Mol. Biol. **607**:73–83.
37. **WHO.** 2010. World malaria report 2010. WHO Press, Geneva, Switzerland.
38. **Wilson, D. W., B. S. Crabb, and J. G. Beeson.** 2010. Development of fluorescent *Plasmodium falciparum* for in vitro growth inhibition assays. Malar. J. **9**:152.

Editor: J. H. Adams

Biochemical and Biophysical Research Communications 414 (2011) 612–617

Contents lists available at SciVerse ScienceDirect

Biochemical and Biophysical Research Communications

journal homepage: www.elsevier.com/locate/ybbrc

Cell-free synthesis, reconstitution, and characterization of a mitochondrial dicarboxylate–tricarboxylate carrier of *Plasmodium falciparum*

Akira Nozawa, Ryoji Fujimoto, Hiroki Matsuoka, Takafumi Tsuboi, Yuzuru Tozawa *

Cell-Free Science and Technology Research Center and Venture Business Laboratory, Ehime University, 3 Bunkyo-cho, Matsuyama, Ehime 790-8577, Japan

ARTICLE INFO

Article history:
Received 24 September 2011
Available online 2 October 2011

Keywords:
Dicarboxylate–tricarboxylate carrier
Membrane protein
Mitochondrial carrier family
Plasmodium falciparum
Cell-free translation system

ABSTRACT

The malaria parasite, *Plasmodium falciparum*, was recently shown to operate a branched pathway of tricarboxylic acid (TCA) metabolism. To identify and characterize membrane transporters required for such TCA metabolism in the parasite, we isolated a cDNA for a dicarboxylate–tricarboxylate carrier homolog (PfDTC), synthesized the encoded protein with the use of a cell-free translation system, and determined the substrate specificity of its transport activity with a proteoliposome reconstitution system. PfDTC was found to mediate efficient oxoglutarate–malate, oxoglutarate–oxaloacetate, or oxoglutarate–oxoglutarate exchange across the liposome membrane. Our results suggest that PfDTC may mediate the oxoglutarate–malate exchange across the inner mitochondrial membrane required for the branched pathway of TCA metabolism in the malaria parasite.

1. Introduction

Most organisms have evolved a canonical cyclic pathway of tricarboxylic acid (TCA) metabolism, although there are some exceptions [1]. For example, the malaria parasite, *Plasmodium falciparum*, was recently shown to operate a noncanonical branched-type TCA metabolic pathway in its mitochondria [2]. It was suggested that this protozoan does not depend on TCA metabolism for the generation of ATP, but rather relies on its unique TCA metabolism for more limited functions such as provision of a precursor, succinyl-CoA, for heme biosynthesis [2]. The starting substrate and end product of the branched TCA metabolism were proposed to be oxoglutarate and malate, respectively. It is therefore important to clarify the transporter function that facilitates efficient uptake of oxoglutarate and removal of malate across the mitochondrial inner membrane (IM).

The transport of molecules across the mitochondrial IM is highly selective, so that an effective barrier exists between the cytosol and the mitochondrial matrix. Members of the mitochondrial carrier family (MCF) of proteins, which is the largest family of transporters, facilitate the selective transport of most solutes across the IM [3]. Analysis of the genome database for *P. falciparum* suggested that it encodes nine MCF homologs [4], with one MCF-like protein being predicted to transport tricarboxylic or dicarboxylic acid intermediates of the TCA pathway [2].

One of the bottlenecks in biochemical analysis of *P. falciparum* proteins has been the lack of an efficient method for protein preparation. The parasite has one of the most A/T-rich genomes known (76.3% in exon regions) [4], with the A/T-biased codon usage having been assumed to affect the expression of encoded proteins in bacterial recombinant systems. A wheat germ cell-free (CF) system was recently shown to be a promising alternative for the production of *P. falciparum* proteins [5]. CF systems also provide an effective tool for the production of transmembrane proteins (TMPs) [6,7], with a variety of modified CF synthesis methods for TMP production having been described [8–11]. An apicoplast phosphate translocator from *P. falciparum* has been synthesized and characterized with the use of a CF system [12].

To gain insight into TCA metabolism in the mitochondria of *P. falciparum*, we have now isolated and characterized a predicted dicarboxylate–tricarboxylate carrier (DTC) homolog of this parasite with the use of a liposome-supplemented CF system. We clarified the substrate specificity of this protein, designated PfDTC, which has implications for the nature of the TCA pathway in the parasite.

2. Materials and methods

2.1. Plasmid construction

Complementary DNA fragments encoding PfDTC (PlasmoDB ID: PF08_0031) and AtDTC (TAIR ID: AT5G19760) were amplified by

Abbreviations: CF, cell-free; DGU, density gradient ultracentrifugation; DTC, dicarboxylate–tricarboxylate carrier; GFP, green fluorescent protein; IM, inner membrane; MCF, mitochondrial carrier family; PAGE, polyacrylamide gel electrophoresis; PCR, polymerase chain reaction; TCA, tricarboxylic acid; TMP, transmembrane protein.

* Corresponding author. Fax: +81 89 927 8528.
E-mail address: tozawa.yuzuru.mx@ehime-u.ac.jp (Y. Tozawa).

0006-291X/$ - see front matter © 2011 Elsevier Inc. All rights reserved.
doi:10.1016/j.bbrc.2011.09.130

the polymerase chain reaction (PCR) from a cDNA prepared from *P. falciparum* parasite rich in schizonts [5] or *Arabidopsis thaliana*, respectively, with the primer sets PfDTC-SpeI (5′-CCACTAGTAACA ATGGACAGAGATATAGCTAAATATG-3′) and PfDTC-SalI (5′-CCGTCG ACTTAAGAAATTTTTTTTAAAAGATTAT-3′) for PfDTC and AtDTC-SpeI (5′-CGACTAGTAACAATGGCGGAAGAGAAGAAAGCT-3′) and At DTC-SalI (5′-GCGTCGACTCACATACCAATCTTCTTTTGAAA-3′) for AtDTC. The PCR products were digested with SpeI and SalI and then cloned into the corresponding sites of the pYT08 vector (Supplementary Materials and methods), yielding pYT08-PfDTC and pYT08-AtDTC, respectively.

2.2. CF protein synthesis

Messenger RNA was prepared by in vitro transcription with pYT08-PfDTC and pYT08-AtDTC as templates. The translation reaction was performed with a wheat germ CF translation system by the bilayer method as described previously [10]; the 25-μl translation layer was overlaid with a 125-μl substrate layer. Acetone-washed asolectin (Fluka, Buchs, Switzerland) was suspended in water and dissolved by ultrasonic treatment for 5 min (30% duty cycle) on ice. The solution was extruded through a polycarbonate membrane with a pore size of 100 nm with the use of a mini-extruder (Avanti Polar Lipids, Alabaster, AL) to form small unilamellar vesicles (liposomes), which were added to the translation layer (final concentration, 0.5 mg/ml). The bilayer reaction was performed at 26 °C for 16 h. The amount of protein synthesized was estimated by measurement of the incorporation of [^{14}C]Leu (100 μCi/ml) (PerkinElmer Japan, Yokohama, Japan) as described previously [13].

2.3. Density gradient ultracentrifugation

Accudenz (Accurate Chemical and Scientific, Westbury, NY) was dissolved in density gradient ultracentrifugation (DGU) solution [30 mM HEPES-KOH (pH 7.8), 100 mM potassium acetate, 2.7 mM magnesium acetate] at concentrations of 30, 35, and 80% (w/v). The translation mixture (150 μl) was mixed with 150 μl of DGU solution and 300 μl of 80% Accudenz solution. The resultant 40% Accudenz solution containing synthesized protein was placed in the bottom of a centrifuge tube and overlaid with 650 μl of 35% Accudenz solution, 650 μl of 30% Accudenz solution, and 100 μl of DGU solution. The gradient was centrifuged at 206,000×*g* for 1 h at 4 °C in a Hitachi S55S rotor (Hitachi High-Technology, Tokyo, Japan). Fractions were then collected from the top of the tube and analyzed by SDS–polyacrylamide gel electrophoresis (PAGE) and autoradiography.

2.4. Reconstitution of synthesized proteins into liposomes and measurement of transport activity

The translation mixture was centrifuged (20,000×*g* for 20 min at 4 °C), and the resulting pellet was resuspended in 10 mM PIPES–NaOH (pH 6.5) and dissolved by ultrasonic treatment for 18 s (50% duty cycle). Substrate-loaded liposomes (final concentration, 80 mg/ml) were prepared from acetone-washed asolectin by ultrasonic treatment for 5 min on ice in a solution containing 200 mM PIPES–NaOH (pH 6.5), 40 mM potassium gluconate, and 60 mM substrate. The dissolved pellet fraction was mixed with an equal volume of the substrate-loaded liposomes, frozen in liquid nitrogen, thawed at room temperature, and subjected to ultrasonic treatment for 18 s (50% duty cycle). Substrate that remained outside of the resultant proteoliposomes was removed with the use of a Dowex AG-1X8 column (Bio-Rad, Tokyo, Japan) that had been equilibrated with a solution containing 10 mM PIPES–NaOH (pH 6.5), 40 mM potassium gluconate, and 100 mM sodium gluconate. The proteoliposomes were applied to the column and eluted with the equilibration solution.

Transport reactions were initiated by the addition of 5 μl of [^{14}C]oxoglutarate (PerkinElmer Japan) to 100 μl of proteoliposomes (final substrate concentrations, 30 mM inside and 0.2 mM outside). The assay was performed at 25 °C, and the reaction was terminated by the addition of 15 μl of stop solution (360 mM pyridoxal 5′-phosphate, 64 mM mersalyl acid). Substrate that remained outside of the proteoliposomes was removed with a Dowex AG-1X8 column that had been equilibrated with 200 mM sodium acetate. The radioactivity associated with the eluted proteoliposomes was measured with a liquid scintillation spectrometer. In control samples, the translation reaction was performed without mRNA. Transport activity was calculated from the difference between experimental and control values.

3. Results and discussion

3.1. Isolation of DTC cDNA from P. falciparum

The *P. falciparum* genome has been predicted to encode nine MCF proteins [4], but the detailed sequence information has not yet been released. We therefore surveyed the *P. falciparum* database to identify gene sequences that encode MCF-like proteins and found 12 candidate cDNAs (Table 1). Five of the 12 predicted proteins showed significant sequence similarity to known MCF proteins, whereas the remaining seven gene products could not be assigned to any of the known MCF subfamilies. We next compared the sequences of these protozoan MCF candidates with those of other MCF proteins known to function as transporters for intermediates of TCA metabolism (Fig. 1), including seven proteins from the yeast *Saccharomyces cerevisiae*, six from human (SLC25 family proteins), and five from the plant *A. thaliana* that serve as oxaloacetate (ScOAC1, SLC25A34, SLC25A35), dicarboxylate (DIC, SLC25A10), oxoglutarate (SLC25A11), dicarboxylate–tricarboxylate (DTC), citrate–oxoglutarate (ScYHM2), oxodiadipate (ScODC, SLC25A21), succinate–fumarate (SFC1), and citrate (ScCTP1, SLC25A1) carriers. From this comparative analysis, we extracted two predicted *P. falciparum* proteins, those encoded by PF08_0031 and PFL1145w, as being most phylogenetically related to these MCF carriers (Fig. 1). PF08_0031 had previously been predicted to encode a mitochondrial oxoglutarate–malate translocator of *P. falciparum* [2]. The sequence comparison revealed that the previously characterized MCF protein that showed the greatest similarity to the protein encoded by PF08_0031 was AtDTC (AT5G19760), with an amino acid sequence identity of 52% (Supplementary Fig. S1). The protein encoded by PFL1145w showed the greatest similarity to *S. cerevisiae* YHM2, a citrate–oxoglutarate carrier, with a sequence identity of 34%. As the most likely candidate for encoding a DTC, we isolated a cDNA fragment including the open reading frame of PF08_0031 from a *P. falciparum* cDNA by PCR. The nucleotide sequence of the isolated 954-bp open reading frame was 100% identical to that in the database, with the encoded 318-amino acid polypeptide having a calculated molecular mass of 35.4 kDa. We designated the protein encoded by PF08_0031 as PfDTC (*Plasmodium falciparum* dicarboxylate–tricarboxylate carrier).

3.2. CF synthesis of MCF proteins

To investigate the function of PfDTC, we synthesized the protein with the use of a wheat germ CF translation system and reconstituted it in proteoliposomes for an in vitro transport assay. We also synthesized *A. thaliana* DTC as a control for comparison of its transport activity with that of PfDTC. The cDNAs for PfDTC and AtDTC were cloned into the CF expression plasmid pYT08, and the resultant

Table 1
Plasmodium falciparum MCF-like proteins predicted on the basis of amino acid sequence similarity.

Gene name	Predicted function	Homologous protein (GenBank ID)	References
PFA0415c			
PFD0367w			
PF08_0031	Dicarboxylate–tricarboxylate carrier Dicarboxylate carrier Oxoglutarate carrier	AtDTC (AED92746), AtDIC1 (CAJ86454), AtDIC2 (CAJ86455), AtDIC3 (CAJ86453), ScDIC1 (AAB67266), SLC25A10 (AAH15797), SLC25A11 (CAG33115)	[17–20]
PF08_0093			
PFI0255c			
PFI0425w			
PF10_0051			
PF10_0366	ADP–ATP carrier	AtAAC1 (NP_187470), AtAAC2 (NP_196853), AtAAC3 (NP_194568), AtAAC4 (NP_568345), ScAAC1 (AAA97486), ScAAC2 (NP_009523), ScAAC3 (NP_009642), SLC25A4 (NP_001142), SLC25A5 (AAH68199), SLC25A6 (NP_001627), SLC25A31 (NP_112581)	[21–27]
PFL0110c	Phosphate carrier	AtPiC1 (NP_196908), AtPiC2 (NP_190454), AT2G17270 (NP_179319), ScPIC1 (NP_012611), ScPIC2 (NP_010973), SLC25A3 (AAH15379)	[3,18,28,29]
PFL1145w	Citrate–oxoglutarate carrier	ScYHM2 (Q04013)	[30]
PFL2000w	*S*-Adenosylmethionine carrier	AtSAMC1 (NP_568060), AtSAMC2 (NP_564436), ScSAM5 (AAA64802), SLC25A26 (Q70HW3)	[31–33]
PF13_0359			

The function of *P. falciparum* MCF-like proteins was predicted on the basis of amino acid sequence similarity to *Arabidopsis* (At), yeast (Sc), and human MCF proteins. The sequence similarity was analyzed with the BLAST program [34], and sequences showing >30% identity to the query sequence are listed as homologous proteins with the corresponding database accession number shown in parentheses.

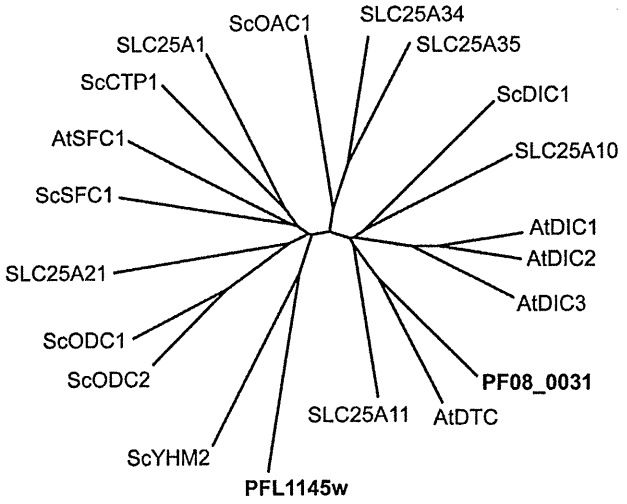

Fig. 1. Phylogenetic relations among MCF proteins. The deduced amino acid sequences of PF08_0031 and PFL1145w from *P. falciparum* were compared with MCF proteins involved in transport of TCA cycle intermediates: ScDIC1, ScODC1 (GenBank ID: NP_015191) [35], ScODC2 (GenBank ID: NP_014865) [35], ScSFC1 (GenBank ID: AAT92943) [36], ScCTP1 (GenBank ID: NP_009850) [37], ScOAC1 (GenBank ID: NP_012802) [38], and ScYHM2 from *Saccharomyces cerevisiae*; AtDTC, AtDIC1, AtDIC2, AtDIC3, and AtSFC1 (GenBank ID: AED90329) [39] from *Arabidopsis thaliana*; and SLC25A1 (GenBank ID: NP_005975) [18], SLC25A10, SLC25A11, SLC25A21 (GenBank ID: EAW65851) [18], SLC25A34 (GenBank ID: NP_997231) [40], and SLC25A35 (GenBank ID: AAI05996) [40] from human. The phylogenetic tree was constructed from the evolutionary distance data derived with the CLUSTAL W program [41].

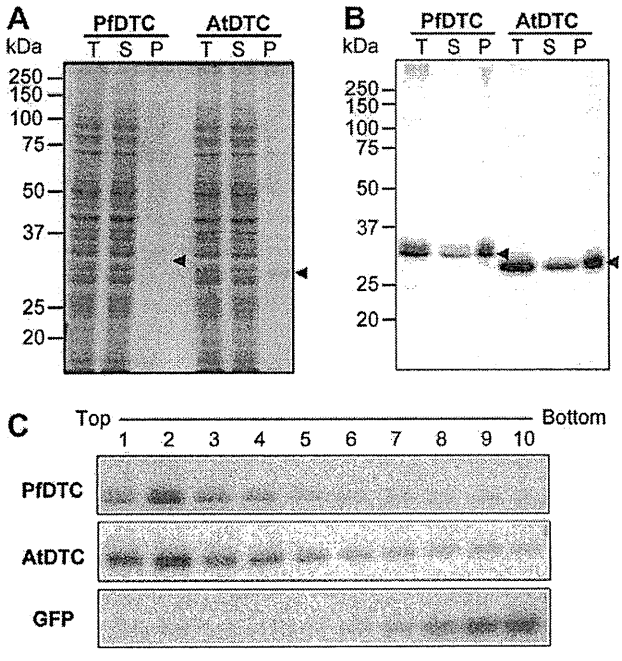

Fig. 2. Synthesis of PfDTC and AtDTC with a CF system. (A) PfDTC and AtDTC were synthesized separately with a wheat germ CF system in the presence of liposomes, and the translation mixture was then centrifuged at 20,000×*g* for 20 min at 4 °C. The total (*T*), soluble (*S*), and pellet (*P*) fractions were subjected to SDS–PAGE and stained with Coomassie brilliant blue. Arrowheads indicate PfDTC and AtDTC. (B) PfDTC and AtDTC synthesized as in (A) but in the additional presence of [^{14}C] Leu were analyzed by centrifugation and SDS–PAGE as in (A) followed by autoradiography. Arrowheads indicate PfDTC and AtDTC. (C) PfDTC, AtDTC, and GFP were synthesized with the CF system in the presence of liposomes and [^{14}C]Leu, and the translation mixture was then subjected to Accudenz DGU. Fractions were collected from the top of the tube and subjected to SDS–PAGE and autoradiography.

plasmids were used in the CF synthesis reaction. Each MCF protein was synthesized in the presence of asolectin liposomes and [^{14}C]Leu, and the labeled proteins were detected and analyzed by SDS–PAGE and autoradiography (Fig. 2A and B). The molecular masses of PfDTC and AtDTC derived from their electrophoretic mobilities were 33 and 31 kDa, respectively, with both proteins migrating as single bands. As with other TMPs, the molecular sizes of the two DTC proteins determined by SDS–PAGE were slightly smaller than those calculated from their predicted amino acid sequences (35.4 kDa for PfDTC and 31.9 kDa for AtDTC). The yields of PfDTC and AtDTC were estimated by measurement of incorporated [^{14}C]Leu and were found to be ~4.6 and 7.6 μg per 150-μl reaction mixture, respectively. The synthesized proteins were present mostly in the pellet fraction of the CF reaction mixture obtained by centrifugation at 20,000×*g* for 20 min at 4 °C (73% of AtDTC and 85% of

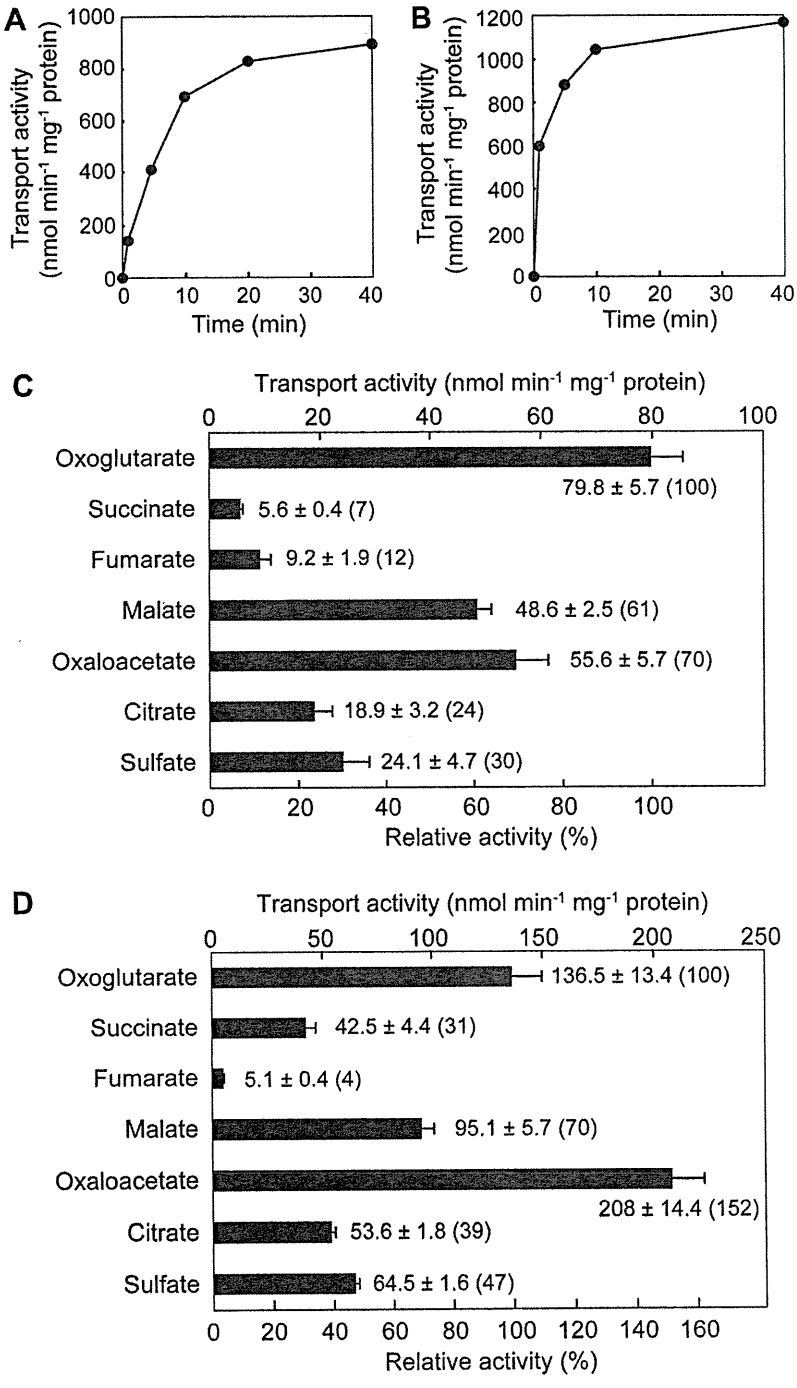

Fig. 3. Substrate transport activity of DTC proteins reconstituted in proteoliposomes. (A and B) Time course of the incorporation of external [^{14}C]oxoglutarate into proteoliposomes reconstituted with PfDTC (A) or AtDTC (B) and loaded with 30 mM oxoglutarate. Data are from representative experiments. (C and D) Substrate specificity of PfDTC (C) or AtDTC (D) for countertransport of oxoglutarate. Proteoliposomes loaded with 30 mM of the indicated substrates were assayed for the uptake of [^{14}C]oxoglutarate over 5 min. Transport activities relative to the corresponding value for oxoglutarate are shown in parentheses. Data are means ± SD from three independent experiments.

PfDTC). The pellets were readily resuspended by the addition of buffer and gentle mixing, suggestive of liposome association of the synthesized proteins [14,15]. We previously found that the *Arabidopsis* phosphate translocator AtPPT1 synthesized with this CF system associated with liposomes during the translation reaction and that the association of TMPs with liposomes is critical for the synthesis of functional proteins [10,13].

We next examined whether the synthesized DTC proteins are indeed associated with the supplemented liposomes. PfDTC, AtDTC, and green fluorescent protein (GFP) were synthesized with the CF system in the presence of liposomes and [^{14}C]Leu. The translation mixtures were then fractionated by Accudenz DGU, during which liposomes migrate to the top layer [16]. Both MCF proteins were detected predominantly in the top layer, whereas GFP, a

control soluble protein, was present in the bottom fractions (Fig. 2C). These results thus showed that the MCF proteins become associated with liposomes during the synthesis reaction.

3.3. Characterization of PfDTC and AtDTC synthesized with the liposome-supplemented wheat germ CF system

To confirm the membrane transporter function of PfDTC, we measured its ability to mediate the exchange of oxoglutarate in comparison with the activity of AtDTC as a positive control. PfDTC and AtDTC were synthesized with the liposome-supplemented CF system and were isolated as proteoliposomes by centrifugation as described above. The pellet fractions were processed in order to reconstitute the synthesized proteins in liposomes loaded with 30 mM unlabeled oxoglutarate. Uptake of [^{14}C]oxoglutarate into the proteoliposomes was then measured. Uptake of [^{14}C]oxoglutarate into the proteoliposomes containing PfDTC or AtDTC proceeded in a time-dependent manner for at least 20 or 10 min, respectively (Fig. 3A and B), showing that both PfDTC and AtDTC were reconstituted in the proteoliposomes as functional membrane transporters.

The oxoglutarate exchange activities of reconstituted PfDTC and AtDTC were calculated as 151 and 600 nmol min^{-1} mg^{-1} protein, respectively, from the experimental data for the reaction time of 1 min. Such activity for AtDTC was previously determined as 1180 nmol min^{-1} mg^{-1} protein [17]. The difference in activity values for AtDTC between this previous and our present study likely reflects differences in experimental conditions. Whereas the internal and external concentrations of substrate in our study were 30 and 0.2 mM, respectively, those in the previous study were 20 and 0.1 mM, respectively [17]. The lipid concentration in the transport assay mixture was also much higher (40 mg/ml) in our study than in the previous study (2.15 mg/ml) [17].

3.4. Substrate specificity of PfDTC

For investigation of the substrate specificity for countertransport by the reconstituted PfDTC, the proteoliposomes containing PfDTC (Fig. 3C) or AtDTC (Fig. 3D) were loaded with different substrates and the uptake of [^{14}C]oxoglutarate was measured. For AtDTC, the highest oxoglutarate uptake activity was apparent with oxaloacetate as the internal substrate, followed by oxoglutarate and malate, and with lower but substantial activity also being observed with sulfate, citrate, or succinate as internal substrates. The countertransport activity of AtDTC for oxoglutarate–fumarate was <2.5% of the oxoglutarate–oxoglutarate exchange activity. The substrate specificity of reconstituted AtDTC in the present study was generally similar to that previously described [17]. Reconstituted PfDTC mediated efficient transport of [^{14}C]oxoglutarate in exchange for oxoglutarate, oxaloacetate, or malate. However, the activity with oxaloacetate relative to that with oxoglutarate for PfDTC was less than half that for AtDTC. Such relative activity for PfDTC proteoliposomes with internal citrate or sulfate was slightly lower than that for AtDTC proteoliposomes, whereas the relative activity for PfDTC proteoliposomes loaded with succinate was much lower than that for AtDTC proteoliposomes. In contrast, the relative countertransport activity with fumarate was threefold as great with PfDTC as with AtDTC. The measured transport activities of reconstituted PfDTC for oxaloacetate, citrate, and succinate in the present study are also lower than those previously determined for AtDTC as well as for *Nicotiana tabacum* DTC1 and DTC3 [17]. It is therefore likely that PfDTC has a more restricted substrate specificity compared with these plant homologs.

Our present experimental and previously reported data together suggest that PfDTC may be specialized to exchange oxoglutarate with malate or oxaloacetate. In mammals, an oxoglutarate–malate carrier as well as an aspartate–glutamate carrier plays a key role in the malate–aspartate NADH shuttle, which transfers reducing equivalents from the cytosol to the mitochondrial matrix for electron transfer [18]. On the other hand, plants do not possess an aspartate–glutamate carrier, with the malate–oxaloacetate exchange mediated by DTC likely contributing to the export of redox equivalents for the production of glycerate during photorespiration [17]. Given that the malaria parasite does not have either an aspartate–glutamate carrier or a photorespiration system, PfDTC function may be important for the efficient exchange of substrates between the cytosol and mitochondrial matrix. Although the transmembrane topology of PfDTC remains to be determined, our data indicate that this protein likely functions in the countertransport of oxoglutarate and malate, which is necessary for the efficient operation of the branched TCA metabolic pathway in *P. falciparum* mitochondria.

Acknowledgments

We thank Y. Endo and other members of the Cell-Free Science and Technology Research Center of Ehime University for support and helpful discussion.

Appendix A. Supplementary data

Supplementary data associated with this article can be found, in the online version, at doi:10.1016/j.bbrc.2011.09.130.

References

[1] T. Mogi, K. Kita, Diversity in mitochondrial metabolic pathways in parasitic protists Plasmodium and Cryptosporidium, Parasitol. Int. 59 (2010) 305–312.
[2] K.L. Olszewski, M.W. Mather, J.M. Morrisey, B.A. Garcia, A.B. Vaidya, J.D. Rabinowitz, M. Llinás, Branched tricarboxylic acid metabolism in *Plasmodium falciparum*, Nature 466 (2010) 774–778.
[3] F. Palmieri, C.L. Pierri, A. De Grassi, A. Nunes-Nesi, A.R. Fernie, Evolution, structure and function of mitochondrial carriers: a review with new insights, Plant J. 66 (2011) 161–181.
[4] M.J. Gardner, H. Hall, E. Fung, O. White, M. Berriman, R.W. Hyman, J.M. Carlton, A. Pain, K.E. Nelson, S. Bowman, I.T. Paulsen, K. James, J.A. Eisen, K. Rutherford, S.L. Salzberg, A. Craig, S. Kyes, M.S. Chan, V. Nene, S.J. Shallom, B. Suh, J. Peterson, S. Angiuoli, M. Pertea, J. Allen, J. Selengut, D. Haft, M.W. Mather, A.B. Vaidya, D.M. Martin, A.H. Fairlamb, M.J. Fraunholz, D.S. Roos, S.A. Ralph, G.I. McFadden, L.M. Cummings, G.M. Subramanian, C. Mungall, J.C. Venter, D.J. Carucci, S.L. Hoffman, C. Newbold, R.W. Davis, C.M. Fraser, B. Barrell, Genome sequence of the human malaria parasite *Plasmodium falciparum*, Nature 419 (2002) 498–511.
[5] T. Tsuboi, S. Takeo, H. Iriko, L. Jin, M. Tsuchimochi, S. Matsuda, E.T. Han, H. Otsuki, O. Kaneko, J. Sattabongkot, R. Udomangpetch, T. Sawasaki, M. Torii, Y. Endo, Wheat germ cell-free system-based production of malaria proteins for discovery of novel vaccine candidates, Infect. Immun. 76 (2008) 1702–1708.
[6] L. Liguori, B. Marques, A. Villegas-Méndez, R. Rothe, J.L. Lenormand, Production of membrane proteins using cell-free expression systems, Expert Rev. Proteomics 4 (2007) 79–90.
[7] D. Schwarz, V. Dötsch, F. Bernhard, Production of membrane proteins using cell-free expression systems, Proteomics 8 (2008) 3933–3946.
[8] C. Klammt, F. Löhr, B. Schäfer, W. Haase, V. Dötsch, H. Rüterjans, C. Glaubitz, F. Bernhard, High level cell-free expression and specific labeling of integral membrane proteins, Eur. J. Biochem. 271 (2004) 568–580.
[9] R. Kalmbach, I. Chizhov, M.C. Schumacher, T. Friedrich, E. Bamberg, M. Engelhard, Functional cell-free synthesis of a seven helix membrane protein: in situ insertion of bacteriorhodopsin into liposomes, J. Mol. Biol. 371 (2007) 639–648.
[10] A. Nozawa, H. Nanamiya, T. Miyata, N. Linka, Y. Endo, A.P.M. Weber, Y. Tozawa, A cell-free translation and proteoliposome reconstitution system for functional analysis of plant solute transporters, Plant Cell Physiol. 48 (2007) 1815–1820.
[11] T. Genji, A. Nozawa, Y. Tozawa, Efficient production and purification of functional bacteriorhodopsin with a wheat-germ cell-free system and a combination of Fos-choline and CHAPS detergents, Biochem. Biophys. Res. Commun. 400 (2010) 638–642.
[12] L. Lim, M. Linka, KA. Mullin, A.P.M. Weber, G.I. McFadden, The carbon and energy sources of the non-photosynthetic plastid in the malaria parasite, FEBS Lett. 584 (2010) 549–554.
[13] A. Nozawa, T. Ogasawara, S. Matsunaga, T. Iwasaki, T. Sawasaki, Y. Endo, Production and partial purification of membrane proteins using a liposome-supplemented wheat cell-free translation system, BMC Biotechnol. 11 (2011) 35.

[14] I. Guilvout, M. Chami, C. Berrier, A. Ghazi, A. Engel, A.P. Pugsley, N. Bayan, In vitro multimerization and membrane insertion of bacterial outer membrane secretin PulD, J. Mol. Biol. 382 (2008) 13–23.
[15] C. Berrier, I. Guilvout, N. Bayan, K.H. Park, A. Mesneau, M. Chami, A.P. Pugsley, A. Ghazi, Coupled cell-free synthesis and lipid vesicle insertion of a functional oligomeric channel MscL, Biochim. Biophys. Acta 1808 (2011) 41–46.
[16] P. Sobrado, M.A. Goren, D. James, C.K. Amundson, B.G. Fox, A protein structure initiative approach to expression, purification, and in situ delivery of human cytochrome b5 to membrane vesicles, Protein Expr. Purif. 58 (2008) 229–241.
[17] N. Picault, L. Palmieri, I. Pisano, M. Hodges, F. Palmieri, Identification of a novel transporter for dicarboxylates and tricarboxylates in plant mitochondria, J. Biol. Chem. 277 (2002) 24204–24211.
[18] F. Palmieri, The mitochondrial transporter family (SLC25): physiological and pathological implications, Pflugers Arch.–Eur. J. Physiol. 447 (2004) 689–709.
[19] L. Palmieri, N. Picault, R. Arrigoni, E. Besin, F. Palmieri, M. Hodges, Molecular identification of three *Arabidopsis thaliana* mitochondrial dicarboxylate carrier isoforms: organ distribution, bacterial expression, reconstitution into liposomes and functional characterization, Biochem. J. 410 (2008) 621–629.
[20] L. Palmieri, F. Palmieri, M.J. Runswick, J.E. Walker, Identification by bacterial expression and functional reconstitution of the yeast genomic sequence encoding the mitochondrial dicarboxylate carrier protein, FEBS Lett. 399 (1996) 299–302.
[21] I. Haferkamp, J.H. Hackstein, F.G. Voncken, G. Schmit, J. Tjaden, Functional integration of mitochondrial and hydrogenosomal ADP/ATP carriers in the *Escherichia coli* membrane reveals different biochemical characteristics for plants, mammals and anaerobic chytrids, Eur. J. Biochem. 269 (2002) 3172–3181.
[22] M. Leroch, H.E. Neuhaus, S. Kirchberger, S. Zimmermann, M. Melzer, J. Gerhold, J. Tjaden, Identification of a novel adenine nucleotide transporter in the endoplasmic reticulum of *Arabidopsis*, Plant Cell 20 (2008) 438–451.
[23] G.S. Adrian, M.T. McCammon, D.L. Montgomery, M.G. Douglas, Sequences required for delivery and localization of the ADP/ATP translocator to the mitochondrial inner membrane, Mol. Cell. Biol. 6 (1986) 626–634.
[24] J.E. Lawson, M.G. Douglas, Separate genes encode functionally equivalent ADP/ATP carrier proteins in *Saccharomyces cerevisiae*. Isolation and analysis of AAC2, J. Biol. Chem. 263 (1988) 14812–14818.
[25] J. Kolarov, N. Kolarova, N. Nelson, A third ADP/ATP translocator gene in yeast, J. Biol. Chem. 265 (1990) 12711–12716.
[26] C. De Macros Lousa, V. Trézéguet, A.C. Dianoux, G. Brandolin, G.J. Lauquin, The human mitochondrial ADP/ATP carriers: kinetic properties and biogenesis of wild-type and mutant proteins in the yeast *S. cerevisiae*, Biochemistry 41 (2002) 14412–14420.
[27] T. Hamazaki, W.Y. Leung, B.D. Cain, D.A. Ostrov, P.E. Thorsness, N. Terada, Functional expression of human adenine nucleotide translocase 4 in *Saccharomyces cerevisiae*, PLoS One 6 (2011) e19250.
[28] P. Hamel, Y. Saint-Georges, B. de Pinto, N. Lachacinski, N. Altamura, G. Dujardin, Redundancy in the function of mitochondrial phosphate transport in *Saccharomyces cerevisiae* and *Arabidopsis thaliana*, Mol. Microbiol. 51 (2004) 307–317.
[29] H. Wohlrab, C. Briggs, Yeast mitochondrial phosphate transport protein expressed in *Escherichia coli*. Site-directed mutations at threonine-43 and at a similar location in the second tandem repeat (isoleucine-141), Biochemistry 33 (1994) 9371–9375.
[30] A. Castegna, P. Scarcia, G. Agrimi, L. Palmieri, H. Rottensteiner, I. Spera, L. Germinario, F. Palmieri, Identification and functional characterization of a novel mitochondrial carrier for citrate and oxoglutarate in *Saccharomyces cerevisiae*, J. Biol. Chem. 285 (2010) 17359–17370.
[31] L. Palmieri, R. Arrigoni, E. Blanco, F. Carrari, M.I. Zanor, C. Studart-Guimaraes, A.R. Fernie, F. Palmieri, Molecular identification of an *Arabidopsis* S-adenosylmethionine transporter. Analysis of organ distribution, bacterial expression, reconstitution into liposomes, and functional characterization, Plant Physiol. 142 (2006) 855–865.
[32] C.M. Marobbio, G. Agrimi, F.M. Lasorsa, F. Palmieri, Identification and functional reconstitution of yeast mitochondrial carrier for S-adenosylmethionine, EMBO J. 22 (2003) 5975–5982.
[33] G. Agrimi, M.A. Di Noia, C.M. Marobbio, G. Fiermonte, F.M. Lasorsa, F. Palmieri, Identification of the human mitochondrial S-adenosylmethionine transporter: bacterial expression, reconstitution, functional characterization and tissue distribution, Biochem. J. 379 (2004) 183–190.
[34] S.F. Altschul, W. Gish, W. Miller, E.W. Myers, D.J. Lipman, Basic local alignment search tool, J. Mol. Biol. 215 (1990) 403–410.
[35] G. Fiermonte, V. Dolce, L. Palmieri, M. Ventura, M.J. Runswick, F. Palmieri, J.E. Walker, Identification of the human mitochondrial oxodicarboxylate carrier. Bacterial expression, reconstitution, functional characterization, tissue distribution, and chromosomal location, J. Biol. Chem. 276 (2001) 8225–8230.
[36] L. Palmieri, F.M. Lasorsa, A. De Palma, F. Palmieri, M.J. Runswick, J.E. Walker, Identification of the yeast ACR1 gene product as a succinate–fumarate transporter essential for growth on ethanol or acetate, FEBS Lett. 417 (1997) 114–118.
[37] R.S. Kaplan, J.A. Mayor, D.A. Gremse, D.O. Wood, High level expression and characterization of the mitochondrial citrate transport protein from the yeast *Saccharomyces cerevisiae*, J. Biol. Chem. 270 (1995) 4108–4114.
[38] L. Palmieri, A. Vozza, G. Agrimi, V. De Marco, M.J. Runswick, F. Palmieri, J.E. Walker, Identification of the yeast mitochondrial transporter for oxaloacetate and sulfate, J. Biol. Chem. 274 (1999) 22184–22190.
[39] E. Catoni, R. Schwab, M. Hilpert, M. Desimone, R. Schwacke, U.I. Flügge, K. Schumacher, W.B. Frommer, Identification of an *Arabidopsis* mitochondrial succinate–fumarate translocator, FEBS Lett. 534 (2003) 87–92.
[40] C.M.T. Marobbio, G. Giannuzzi, E. Paradies, C.L. Pierri, F. Palmieri, α-Isopropylmalate, a leucine biosynthesis intermediate in yeast, is transported by the mitochondrial oxaloacetate carrier, J. Biol. Chem. 283 (2008) 28445–28453.
[41] J.D. Thompson, D.G. Higgins, T.J. Gibson, CLUSTAL W: improving the sensitivity of progressive multiple sequence alignment through sequence weighting, position specific gap penalties and weight matrix choice, Nucleic Acids Res. 22 (1994) 4673–4680.

Vaccine 29 (2011) 9038–9050

Contents lists available at SciVerse ScienceDirect

Vaccine

journal homepage: www.elsevier.com/locate/vaccine

Immunogenicity of novel nanoparticle-coated MSP-1 C-terminus malaria DNA vaccine using different routes of administration

Mahamoud Sama Cherif[a,c,e], Mohammed Nasir Shuaibu[a,c], Tomoaki Kurosaki[b], Gideon Kofi Helegbe[a], Mihoko Kikuchi[a], Tetsuo Yanagi[d], Takafumi Tsuboi[f], Hitoshi Sasaki[b,c], Kenji Hirayama[a,c,*]

[a] Department of Immunogenetics, Institute of Tropical Medicine (NEKKEN), Nagasaki University 1-12-4 Sakamoto, 852-8523, Japan
[b] Department of Hospital Pharmacy; Nagasaki University. 1-7-1 Sakamoto, 852-8501, Japan
[c] Global COE program, Institute of Tropical Medicine (NEKKEN), Nagasaki University 1-12-4 Sakamoto, 852-8523, Japan
[d] Animal Research Center for Tropical Medicine, Nagasaki University 1-12-4 Sakamoto, 852-8523, Japan
[e] Institut National de Santé Publique (INSP), BP: 6623-Conakry & Université de Conakry, BP: 1147, Conakry, Guinea
[f] Cell-Free Science and Technology Research Center, Ehime University, Matsuyama, Ehime 790-8577, Japan

ARTICLE INFO

Article history:
Received 5 August 2011
Received in revised form 31 August 2011
Accepted 9 September 2011
Available online 20 September 2011

Keywords:
Malaria
DNA vaccine
MSP1
Nanoparticle
Delivery system
Routes administration

ABSTRACT

An important aspect in optimizing DNA vaccination is antigen delivery to the site of action. In this way, any alternative delivery system having higher transfection efficiency and eventual superior antibody production needs to be further explored. The novel nanoparticle, pDNA/PEI/γ-PGA complex, is one of a promising delivery system, which is taken up by cells and is shown to have high transfection efficiency. The immunostimulatory effect of this novel nanoparticle (NP) coated plasmid encoding *Plasmodium yoelii* MSP1-C-terminus was examined. Groups of C57BL/6 mice were immunized either with NP-coated MSP-1 plasmid, naked plasmid or NP-coated blank plasmid, by three different routes of administration; intravenous (i.v.), intraperitoneal (i.p.) and subcutaneous (s.c). Mice were primed and boosted twice at 3-week intervals, then challenged 2 weeks after; and 100%, 100% and 50% mean of survival was observed in immunized mice with coated DNA vaccine by i.p., i.v. and s.c., respectively. Coated DNA vaccine showed significant immunogenicity and elicited protective levels of antigen specific IgG and its subclass antibody, an increased proportion of $CD4^+$ and $CD8^+$ T cells and INF-γ and IL-12 levels in the serum and cultured splenocyte supernatant, as well as INF-γ producing cells in the spleen. We demonstrate that, NP-coated MSP-1 DNA-based vaccine confers protection against lethal *P. yoelii* challenge in murine model across the various route of administration and may therefore, be considered a promising delivery system for vaccination.

1. Introduction

Malaria is a major cause of disease and death, with half of the world's population at risk [1], and an estimated 243 million cases led to nearly 863,000 deaths in 2008 and most of them are children under 5 years of age [2,3]. Various strategies have been developed to prevent this burden, such as diagnosis and treatment, and vector control [4–6]. However, these strategies are still limited because of malaria parasite resistance to most antimalarial drugs and insecticide resistance in the anopheline mosquitoes that transmit the disease [5,7]. Together with other control methods, vaccination holds the promise of controlling and perhaps eventually eradicating malaria [8–11]. DNA vaccination is one of the novel approaches for developing new generation vaccines against malaria. Blood stage infection is established by the invasion of erythrocytes by merozoites [12,13], and a great deal of effort is focused on vaccines targeting this stage, because this approach can directly reduce morbidity and mortality associated with malarial disease in humans [14]. Hence, any intervention that could block merozoite invasion of erythrocyte can lead to control of malaria parasite replication [15,16]. Of the many proteins associated with merozoite, merozoite surface protein 1 (MSP-1), has become a major vaccine candidate [17,18]. This is because antibodies to MSP-1 C-terminal portion, was found at all stages of invasion from initial attachment through to complete invasion [13,19], and therefore considered a promising candidate for the development of a malaria vaccine [20].

Major problems and difficulties associated with malaria vaccine development have been highlighted [21–23], and one of them is the poor immunogenicity of genetically engineered

* Corresponding author at: Department of Immunogenetics, Institute of Tropical Medicine (NEKKEN), Nagasaki University 1-12-4 Sakamoto, 852-8523, Japan. Tel.: +81 95 819 7818; fax: +81 95 819 7821.
E-mail addresses: hiraken@nagasaki-u.ac.jp, nshuaibu@yahoo.com (K. Hirayama).

0264-410X/$ – see front matter © 2011 Elsevier Ltd. All rights reserved.
doi:10.1016/j.vaccine.2011.09.031

antigens, and which required a delivery system and adjuvant to elicit their effect at targeted site of action. A delivery system which transports the antigen to site of action with an adjuvant that activates the cells via interaction with cell receptors and enhances the potency of the antigen, are important aspect in optimizing DNA vaccination [23–25]. Introduction of nanotechnology and the development of nano-carrier-based vaccines have started to receive a lot of attention in order to provide effective immunization through better targeting and triggering antibody response at the cellular level. Many studies demonstrated that, non-viral carrier systems are widely used as transfection agents to deliver nucleic acids for both in vitro and in vivo applications [26,27]. Recently, a few nanoparticle-based vaccines have shown to be effective in the induction of immune responses in animal models without the need for an adjuvant [28]. In this way, any alternative gene delivery systems having higher transfection efficiency and eventual superior antibody production needs to be further explored. The novel nanoparticle (pDNA/-PEI/γ-PGA complex) is one of the promising gene delivery system, which is taken by the cells via γ-PGA-specific receptor mediated pathway and showed high transfection efficiency and low toxicity [29]. Recently, application of this nanoparticle coating MSP-1 by intravenous delivery was shown to partially protect against lethal *Plasmodium yoelii* challenge in mouse model [30]. Also, in the past several years, attention was placed on routes of vaccine administration in order to induce strong immune response against pathogens. The choice of routes to deliver plasmid DNA for obtaining efficacious immunogenic response of the expressed antigen is restricted [31–34] and also influences the immune responses [32,33,35–37]. Therefore, determination of optimal routes to induce antibody and cellular responses are important steps in the development of vaccines against malaria infection.

It is because of the need for an improved delivery system, that in this study, we used nanoparticle formulation for the delivery of a characterized malaria blood stage vaccine candidate (MSP-1). The aim of this current study was to check the effect of nanoparticle coating on *P. yoelii* MSP-1 C-terminus plasmid on induction of immune response in mice using three different routes of administration.

2. Materials and methods

2.1. Construction and purification of MSP1-C terminus plasmid DNA

Sequence of *P. yoelii* MSP-1 (*PY05748*) from the *Plasmodium* genome database, PlasmoDB (www.plasmodb.com) was used for primer design. Primer set of MSP-1 fragment from region 4819–5286 bp, with BglII and BamHI restriction sites, were designed using Oligo Perfect™ Designer (www.invitrogen.com). Forward-5′-***AGATCT***ATGCTTGACGAATTTGTAGAACATGC-3′ and reverse 3′-***GGATCC***CTTATAATAAAATTGATAATCCCATAAAGCT-5′ (restriction sites underlined). *P. yoelii* blood-stage cDNA was used as template to PCR amplify the C-terminal MSP-1. The PCR-amplified product was directly cloned into a BglII and BamHI restriction sites of plasmid VR1020 (Vical, San Diego, CA) to obtain the construct pVR1020-MSP-1 C-terminus. Plasmid DNA, pVR1020-MSP-1 C-terminus was transformed into Top10 chemically competent *Escherichia coli* (Invitrogen, Carlsbad, CA). Ten (10) bacterial colonies were picked and plasmid purified using Qiagen miniprep kits (Qiagen, Maryland) to check the presence of expected fragment. The plasmid containing expected inserts were analyzed by restriction digestion and DNA sequence in the constructs was confirmed by automated DNA sequencing. For large scale DNA vaccine preparation, the plasmid DNA was purified using Qiagen Mega kits (Qiagen, Maryland, USA) according to the manufacturer's instructions. The purified plasmid DNA was resuspended in 5% glucose solution in appropriate concentration and kept until use at −80 °C.

2.2. Formulation and preparation of nanoparticle pDNA complex

Nanoparticle (PEI/γ-PGA) coated-plasmids were formulated as previously described [29]. Briefly, polyethylenimine (PEI) solution (pH 7.4) and pDNA, pVR1020-MSP-1 C-terminus or pVR1020 blank, were mixed by pipetting thoroughly and left for 15 min at room temperature and then gamma polyglutamic acid (γ-PGA) was mixed with the pDNA/PEI complex by pipetting and incubated at room temperature for 15 min. The ternary complex, pDNA/PEI/γ-PGA was constructed at a charge ratio, phosphate of pDNA:nitrogen of PEI:carboxylate of γ-PGA = 1:8:6, with 62.8 ± 0.3 nm particle size and − 14.8 ± 0.7 mV electric charge (ζ-potential). The size and ζ-potential of the complex was determined using Zetasizer Nano ZS (Malvern Instrument, Ltd., UK).

2.3. Immunization of mice

Three different routes of injection; intravenous (i.v.), intraperitoneal (i.p.) and subcutaneous (s.c.) were used to immunize groups of 6-week-old female C57BL/6 mice (SLC, Lab, Japan) with different formulations of the DNA vaccine designated as coated, naked and coated control. Mice in the coated group were immunized with 100 μg of coated-plasmid DNA (pVR1020-MSP-1/PEI/γ-PGA), naked group with 100 μg of pVR1020-MSP-1 C-terminus, and coated control group with 100 μg of pVR1020/PEI/γ-PGA. In the first experiment, ten (10) C57BL/6 mice were used in two groups, one for coated plasmid DNA and the other for naked, to observe the effect of coating. After the first experiment, we proceeded to the second experiment that was designed to observe the antigen driven immune response after the vaccination with the coated plasmid DNA. Mice were prime-immunized at day 0 and two subsequent boosters of 100 μg/mouse of plasmid DNA were given at day 21 and 42. Two weeks after the last immunization, pooled or individual sera were collected from all the mice, for ELISA and cytokines analysis, and 2 mice from each group were randomly picked and sacrificed and spleen cells prepared for flow cytometric analysis, ELISPOT and cytokines analysis.

2.4. Ethical statement

The study was conducted strictly according to the recommendation in the Fundamental Guidelines for Proper Conduct of Animal Experiment and Related Activities in Academic Research Institutions under the jurisdiction of the Ministry of Education, Culture, Sports, Science and Technology, Japan (Notice no. 71). All animal experiments were approved by the Nagasaki University, Board of Animal Research, according to Japanese Guideline for use of experimental animals (Permit Number 0811130716). All efforts were made to minimize suffering, and animals were humanely sacrificed under ketamine anesthesia.

2.5. Challenge infection and protection assay

Two weeks after the last immunization, mice were each challenged by intraperitoneal injection of 10^5 of lethal strain of *P. yoelii 17XL*-parasitized red blood cells (pRBCs) as described [30]. Blood smears from the tail snips were examined by microscopy for the presence of parasites after staining with Giemsa. Parasitaemia was monitored, from day 4 after challenge infection, daily until clearance of parasitaemia or otherwise death of mouse.

2.6. Parasite antigen preparation and recombinant P. yoelii MSP-1 C-terminus proteins

P. yoelii antigen was prepared as previously described [30]. Briefly, parasite protein extracts were prepared by incubation of *P. yoelii*-infected RBCs in 0.15% saponin in PBS for 30 min and washed 3 times in PBS by centrifuging at 2000 rpm. The parasite pellet was then solubilized in 1% Triton X-100 and the cells were broken by freeze and thaw in liquid nitrogen 3 times. The lysate was then centrifuged at 10,000 × *g* for 10 min and the supernatant was used as soluble lysate or as crude antigen for ELISA. $PyMSP1_{19}$ encompasses C-terminal region of PyMSP1 (Asp1658 to Gly1757) based on the sequence of *P. yoelii* MSP-1 (*PY05748*) was amplified by PCR from *P. yoelii* 17XNL gDNA and cloned between the XhoI and BamHI sites of plasmid pEU-E01-GST-TEV (a vector with an N-terminal glutathione S-transferase tag followed by a tobacco etch virus protease cleavage site; Cell Free Sciences, Matsuyama, Japan). The inserted nucleotide sequence was confirmed using the ABI PRISM 3130 Genetic Analyzer and the BigDye Terminator v1.1 Cycle Sequencing kit (Applied Biosystems, Foster City, CA). Recombinant protein $PyMSP1_{19}$ was produced with the wheat germ cell-free protein expression system by the bilayer translation reaction method described previously [38,39]. After synthesis, the $PyMSP1_{19}$ was affinity purified by passage through a glutathione–sepharose 4B column (GE Healthcare, Camarillo, CA) and eluted by on-column cleavage with AcTEV protease (Invitrogen, Carlsbad, CA) after extensive washing of the column with phosphate-buffered saline (PBS). Concentration of purified protein was determined using the Bradford protein assay kit (Bio-Rad Laboratories, Hercules, CA). Purified protein sample was then stored in aliquots at −80 °C until assayed using enzyme-linked immunosorbent assays (ELISA).

2.7. Measurement of antibodies titre by ELISA

Immunoglobulin G and its subtype antibody responses were assessed by ELISA from the pooled sera collected from immunized mice 14 days after last immunization as described previously [30]. Briefly, 96-well plates were coated with 100 μl of 0.5 μg/ml of rMSP1 C terminus or 18 μg/well of parasite antigen in coating buffer and kept overnight at 4 °C. Plates were washed three times with 400 μl/well of 0.05% Tween–PBS and then blocked for nonspecific binding using 340 μl/well of 0.1% blocking reagent (Roche Diagnostics, Mannheim, Germany) for 1 h at 37 °C. Plates were washed three times with 400 μl/well of 0.05% Tween–PBS and 100 μl of serially diluted pooled sera (1:20) was added and incubated at 37 °C for 3 h. Plates were then washed five (5) times with 400 μl/well of 0.05% Tween–PBS, and 100 μl of horse raddish peroxidase (HRP)-conjugated goat anti-mouse IgG and subclasses (Southern Biotechnology, Birmingham, AL) diluted with blocking buffer (1:4000 and 1:2500 for IgG and subtypes, respectively) was added and incubated for 1 h at room temperature. Plates were washed 5 times with 400 μl/well of 0.05% Tween–PBS and antigen–antibody reaction was visualized by the addition of 50 μl/well of 3, 3′, 5, 5′-tetramethylbenzidine (TMB) (Vector Laboratories, CA, USA). The color development reaction was stopped after 30 min by adding 50 μl of 1 N of H_2SO_4, and the absorbance was measured in an automated plate reader (Bio-Rad, Hercules, CA) at 450 nm.

2.8. Flow cytometric analysis of $CD4^+$ and $CD8^+$ T cells

Spleens were removed aseptically from each mouse and splenocytes prepared using two sterilized slide glass by gently pressing the spleens on the rough edge of the slide to get lymphocytes in 10 ml of RPMI 1640 medium containing 10% fetal calf serum (FCS). This was pipetted several times and filtered through gauze. The filtrate was then centrifuged at 1550 rpm for 5 min with 10% FCS–RPMI. Lysis buffer was added and incubated at room temperature for 15 min, to lyse any trace of red blood cells. After washing, 100 μl containing 1×10^6 splenocytes were prepared and transferred into flow cytometry tubes, stained with Fc-γ blocking antibody, and incubated for 15 min at 4 °C. Washing was done once with 800 μl of wash buffer and centrifuged at 3600 rpm for 90 s. Stained surface molecules (APC-CD3, FITC-CD4 and PE-CD8) for $CD4^+$ and $CD8^+$ T were detected by adding 2 μg/ml/test of APC-conjugated anti-CD3, FITC-conjugated anti-$CD4^+$ or PE-conjugated anti-$CD8^+$ and incubated at 4 °C for 30 min in the dark. Cells were washed twice and resuspended in 500 μl of FACs buffer and acquired on the FACS machine (Beckman Coulter Fullerton, CA, USA). Phenotype analyses were performed using the Kaluza software (BD Biosciences, USA).

2.9. Splenocyte culture supernatant and serum cytokine analyses

Cytokine (IL-4, IL-10, IL-12 and IFN-γ) levels in the supernatants of antigen stimulated splenocyte and sera from immunized mice were measured using Procarta® Cytokine Assay Mouse Plex Kits (Affymetrix, Inc. Santa Clara, CA, USA) in quadruplicate, according to the manufacturer's instructions. Briefly, after standard preparation, filter plate was wet with 150 μl/well of reading buffer and incubated at room temperature for 5 min. Fifty microliters (50 μl/well) of antibody beads were added to each well, and washed once with 150 μl of washing buffer. Twenty five microliter (25 μl/well) of serum standard buffer, and either 25 μl/well of serum samples or 50 μl/well of supernatant were added and incubated at room temperature for 1 h. Plates were washed three times, and 25 μl of premixed detection antibody was added, incubated for 30 min on a shaker at room temperature. After three washes, 50 μl of Streptavidin-PE (Affymetrix, Inc. Santa Clara, CA, USA) was added and incubated for 30 min. Three washes after, 120 μl/well of reading buffer was added to each sample well and read on a Luminex instrument, LABScan 100 (Luminex Corporation. Austin, USA).

2.10. Determination of IFN-γ and IL-4 producing T cells by ELISPOT assay

ELISPOT was carried out in duplicates for activated and non-activated cells using mouse IFN-γ ELISPOT and IL-4 ELISPOT kits (Mabtech AB, Sweden). IFN-γ ELISPOT and IL-4 ELISPOT assays were performed using spleen cells activated with *P. yoelii* antigen according to the manufacturer's instructions. Briefly, splenocytes collected from different group of immunized mice were incubated with 5 μg/ml of *P. yoelii* antigen or 1 μg/ml of concanavalin A (Sigma, USA), and kept at 37 °C in a 5% CO_2 atmosphere either for 24 h (IL4 assay) or 48 h (INF-γ assay). Ninety-six-well Multiscreen-IP membrane plate (MultiScreen, Millipore MAIP S45) was pre-wet with 15 μl of 35% of ethanol for maximum of 1 min. Plates were washed 5 times with 200 μl of sterile water per well and coated either with 100 μl at a concentration of 15 μg/ml of an anti-mouse recombinant IL-4 (11B11) (Mabtech AB, Sweden) or anti-mouse recombinant IFN-γ monoclonal antibody (AN18) (Mabtech AB, Sweden) and incubated at 4 °C overnight. The plate was washed 5 times with 200 μl per well of sterile PBS (pH 7.4). The plates were then blocked by adding 200 μl of 10% FCS–RPMI and incubated at room temperature for 30 min. Two million spleen cells (2×10^6) resuspended in 100 μl/well of serially diluted cell suspension (1:10) was added and incubated at 37 °C in a 5% CO_2 atmosphere overnight. Plates were washed and incubated with peroxidase-conjugated streptavidin diluted in PBS–0.5% FCS (1:800). Seventy-five microliters (75 μl/well) of 1-Step

NBT/BCIP Solution (Pierce, Rockford, IL, USA) was added for spot development, then plates were washed extensively in tap water and left to dry at room temperature before spots counting. All samples were tested in duplicates and each immunization experiment was independently repeated at least two times. Spot counting was done using Eliphoto Scan software (Minerva Tech K.K, Tokyo, Japan).

2.11. Statistical analysis

Data were analyzed with GraphPad prism (Software version 5.00, Inc; San Diego California USA). Survival curves were analyzed using Kaplan–Meier test. The Student *t*-test was used to analyze the difference in antibody response between mice in coated and naked groups. The Pearson rank correlation test was used to determine the relationship between survival rates and different parameters. Statistical significance was designated as $p < 0.05$.

3. Results

3.1. Comparison of the effects of nanoparticle (NP) coated and naked DNA vaccine

3.1.1. On the course of blood-stage infection

To determine whether immunization with nanoparticle-coated MSP-1 C-terminus plasmid have any effect on the course of blood-stage infection, two groups of mice were immunized three (3) times at 3-week intervals with either coated or naked MSP-1 C-terminus plasmid and finally challenged with 10^5 of lethal *P. yoelii 17XL*-parasitized red blood cells intraperitoneally. It was clearly observed that mice immunized with coated plasmid, across of all the 3 routes of immunization, have lower parasitaemia than the naked plasmid vaccinated group (Fig. 1A). Mice immunized with NP-coated MSP-1 C-terminus plasmid survived longer and were protected against lethal strain of *P. yoelii* challenge than those groups immunized with naked plasmid (Fig. 1A). However, mice immunized by s.c. route showed a partial protection with about 57% survival (Table 1).

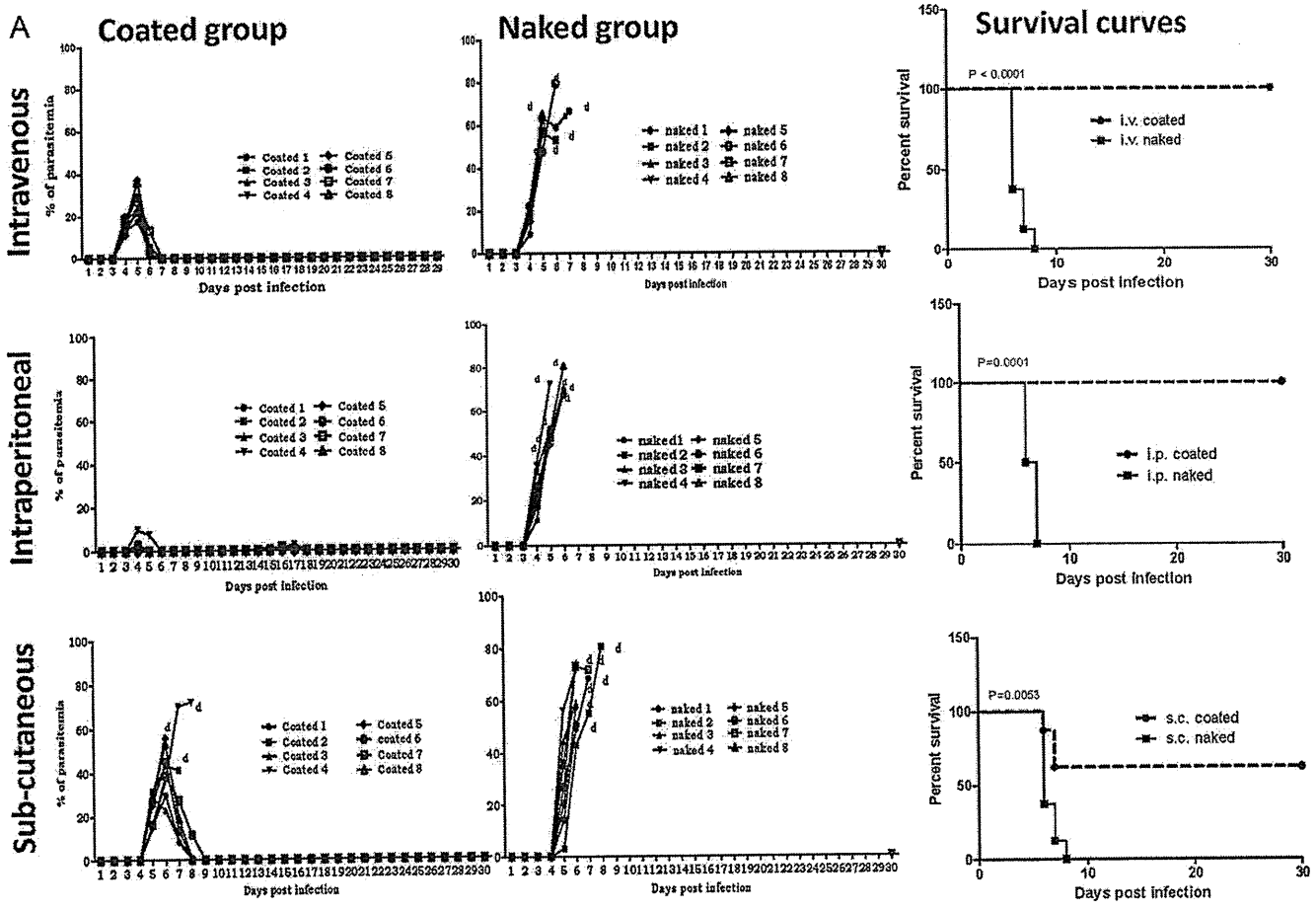

Fig. 1. Effect of coating on the course of parasitaemia and survival curves in group of immunized mice. (A) Parasitaemia profile and survival curve: 6 weeks old C57BL/6 mice were divided in two groups (coated and naked plasmid DNA). Mice were immunized 3 times at 3-week intervals by i.v., i.p. and s.c. routes of administration, then challenged by intraperitoneal injection of 10^5 pRBCs and paraitaemia monitored daily. Each line represents individual mouse with its parasitaemia profile. The notations coated 1–8, naked 1–8 represent individual mouse; d is indicated for death. (B) Stimulatory effect of coating on the course of parasitaemia and survival rates in group of immunized mice. (A) Parasitaemia profile. Six weeks old C57BL/6 mice were divided into two groups; NP-coated plasmid DNA and NP-coated blank plasmid, to observe the effect of coating on antigen driven immune responses. Mice were immunized 3 times at 3-week intervals by i.v., i.p. and s.c. routes of administration, then challenged and parasitaemia monitored daily. Each line represents individual parasitaemia profile. The notations coated 1–6, coated control 1–6 represent individual mouse; d is indicated for death. Survival curves analyzed by using Kaplan–Meier test. Statistical significance was designated as $p < 0.05$.

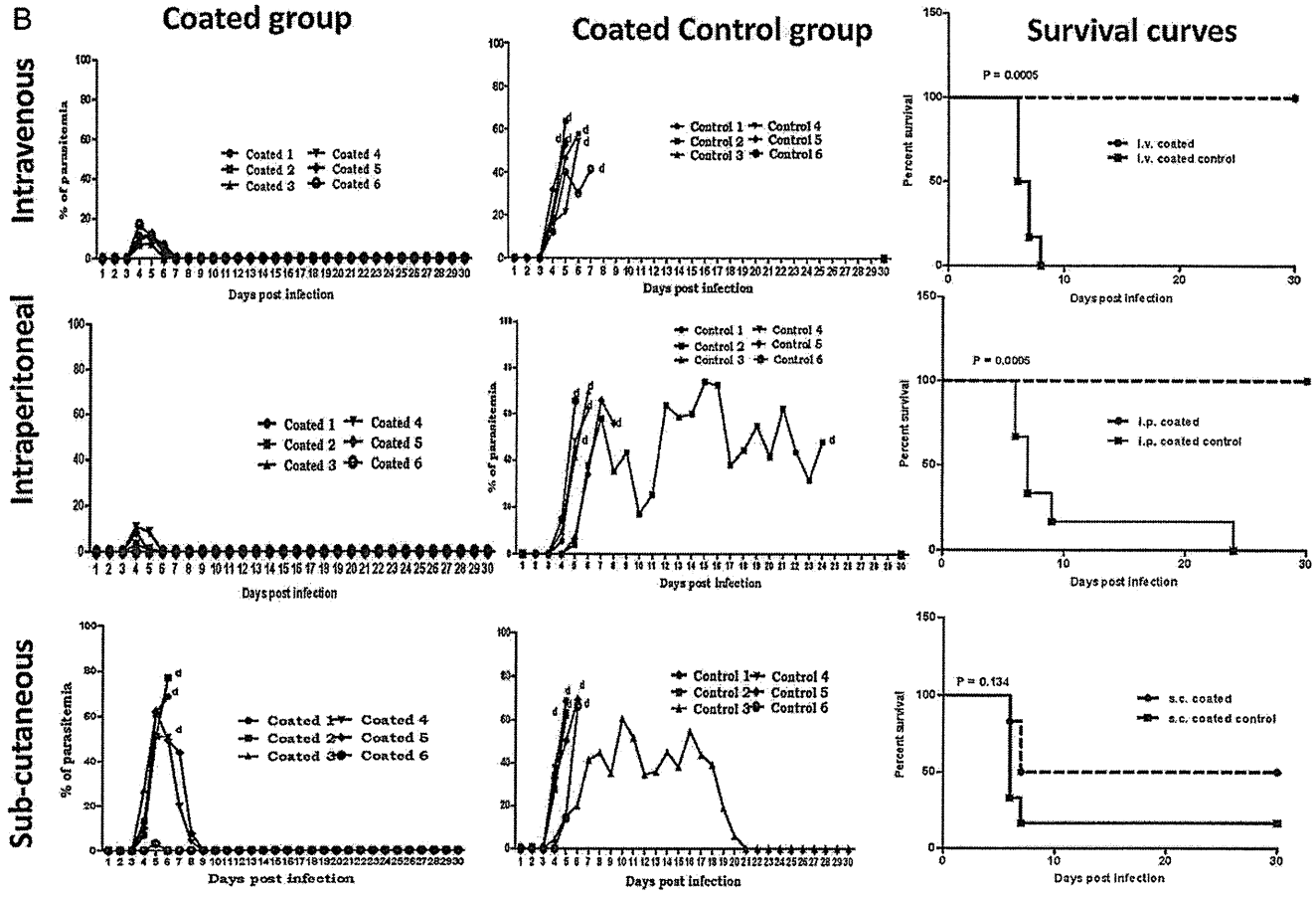

Fig. 1. *Continued.*

3.1.2. On antigen specific IgG and its subclass antibodies production

Sera were collected from immunized mice 2 weeks after the last immunization and recombinant MSP-1 antigen specific IgG and its subclass antibody titers were measured by ELISA. It was clearly observed that group of mice immunized with NP-coated MSP-1 C-terminus plasmid showed high levels of IgG and IgG1, IgG2a and IgG2b subtypes as compared to naked group, regardless of the three routes administered (Fig. 2A and B). To check the variations between individual mouse antibody productions within the group of immunized mice, individual mouse serum was analyzed by ELISA for IgG, IgG1, IgG2a and IgG2b (Fig. 2C). However, mean antibody titers obtained from individual mice and the pooled sera varied, this could be attributable to assay variability. We observed a significant difference of IgG2a and IgG2b subtypes antibody between coated and naked in vaccinated mice by i.p. and i.v. No significant difference was observed between coated and naked in group of mice vaccinated by s.c. route of administration. Similar results were obtained using crude antigen (Fig. S1).

Table 1
Summary of the total number of mice immunized in two different independent experiments depicting the percentage survival.

Routes	Group	Total number of mice	Number of survived	Percentage of survival
i.v.	Coated	14	14	100
	Naked	14	1	7.14
	Coated control	6	0	0
i.p.	Coated	14	14	100
	Naked	14	1	7.14
	Coated control	6	0	0
s.c.	Coated	14	8	57.14
	Naked	14	2	14.28
	Coated control	6	1	16.6

3.1.3. On splenic T cell populations

To check the antigen driven stimulatory effect by the NP-coated DNA vaccine, the number of $CD4^+$ and $CD8^+$ T cells in the spleen were estimated in two mice picked randomly from each group sacrificed 14 days after the last immunization. Flow cytometric analysis was performed on splenocytes by staining with surface molecules (CD3-APC, CD4-FITC and CD8-PE). The percentage of $CD4^+$ and $CD8^+$ T cells was higher in the spleen cells of mice from the coated group as compared naked group across of all the route administration (Fig. 3A).

3.1.4. On cytokines production

To observe the effect of NP coating on cytokine production, four (4) cytokines (IL-4, IL-10, IL-12p40 and IFN-γ) were estimated from cultured splenocyte supernatants and pooled sera from each group of immunized mice. Consistently, it appeared that IL-12p40 production in both serum and culture supernatant was significantly higher in mice immunized with coated DNA plasmid as compared to naked DNA plasmid across of all the three route of delivery. Also, IL-4, IL-10 and INF-γ appeared to be higher in mice immunized intraperitoneally with coated DNA plasmid (Fig. 4A and B).

3.2. Antigen driven immuno-stimulatory effect of NP-coated DNA vaccine compared with NP-coated blank plasmid DNA

On protection, antibody production and T cells proliferation

Two groups of mice were immunized three times at 3 weeks intervals with either coated plasmid or coated blank plasmid and finally challenged with 10^5 pRBCs. It was observed that group of mice immunized with coated MSP-1 plasmid showed low parasitaemia as compared to coated blank plasmid immunized mice (Fig. 1B). After challenge, all the mice in coated groups immunized by i.v. and i.p. were able to control their parasitaemia and recovered completely from lethal challenge, which was similar

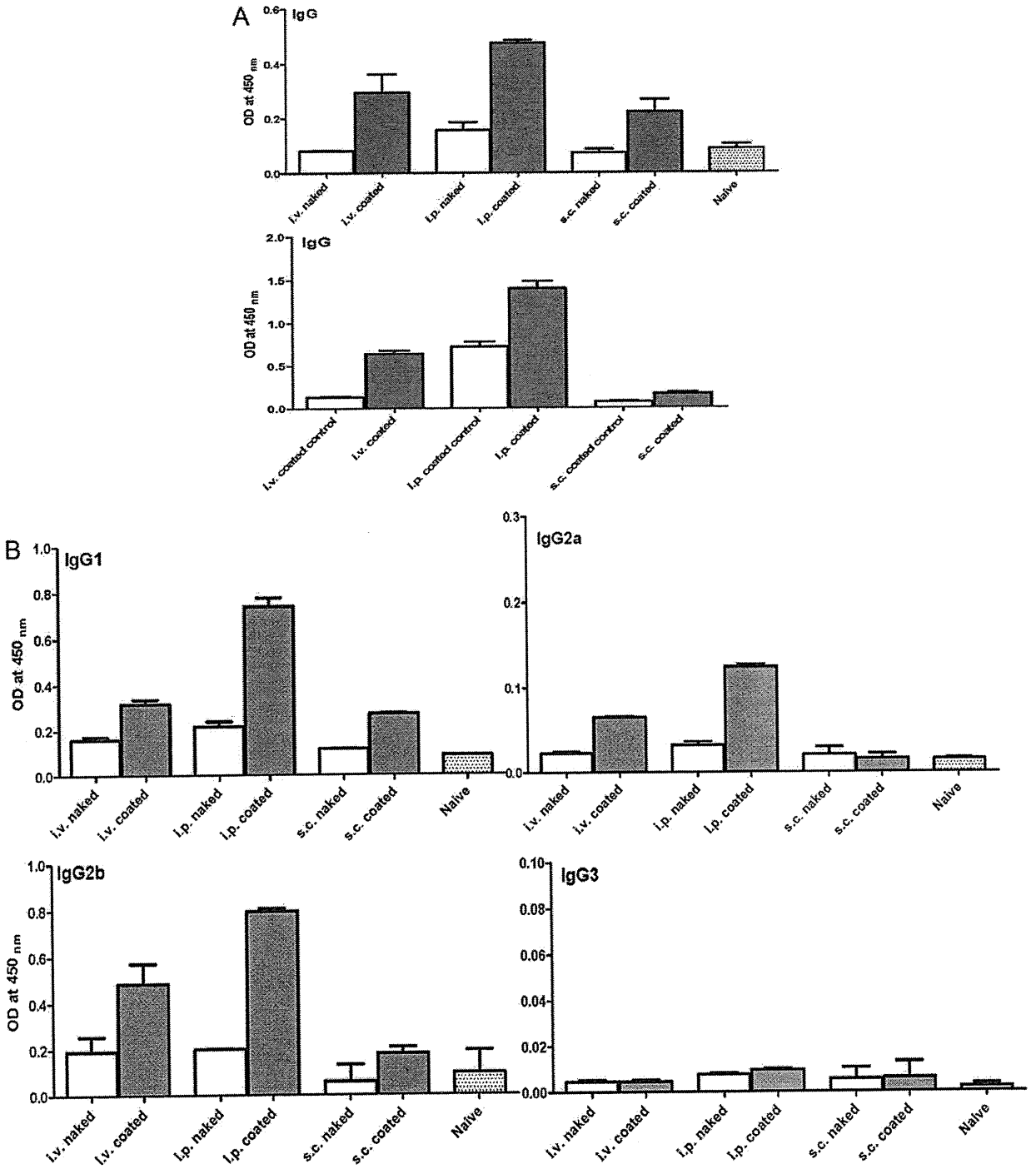

Fig. 2. Stimulatory effect of nanoparticle coating on IgG and its subclass antibody production. Two weeks after the last immunization, sera were collected from immunized mice in each group and IgG levels measured by ELISA as $OD_{450\,nm}$ at 1:40 dilution using rMSP-1. Values are mean ± SD of duplicate measurement. (A) Total IgG antibody titre in the pooled sera collected from immunized mice from the first and second experiment, upper and lower panel, respectively. (B) IgG subclasses antibody titre in the pooled sera collected from immunized mice from the first experiment. (C) Individual IgG and its subclass levels antibody titre in the group of immunized mice with coated plasmid (gray-shaded box plot) or naked (open box plot). Student test was used to find difference between coated and naked group. Statistical significance was designated as $p < 0.05$. (D) IgG subclasses antibody titre in the pooled sera collected from immunized mice from the second experiment.

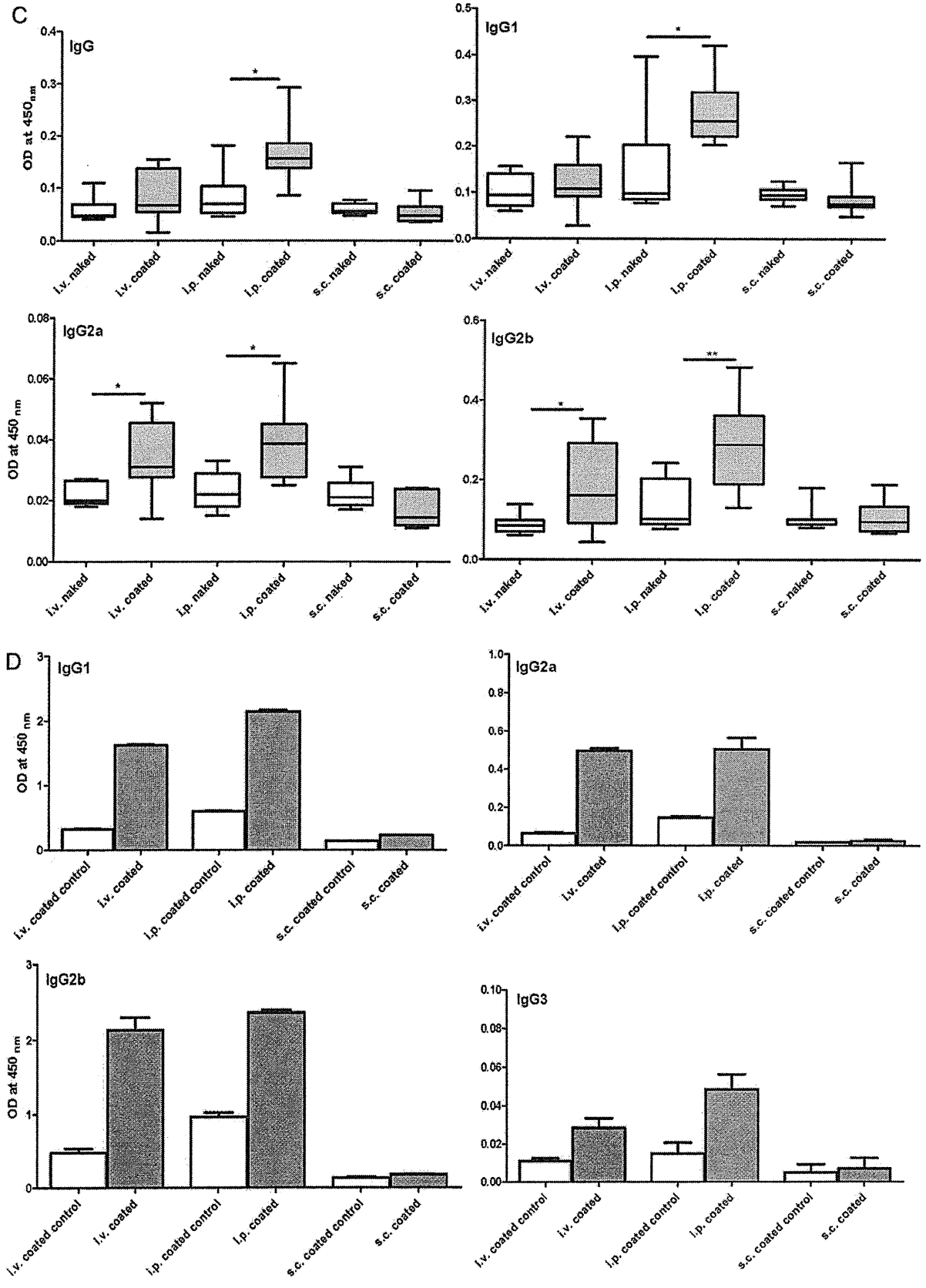

Fig. 2. *Continued.*

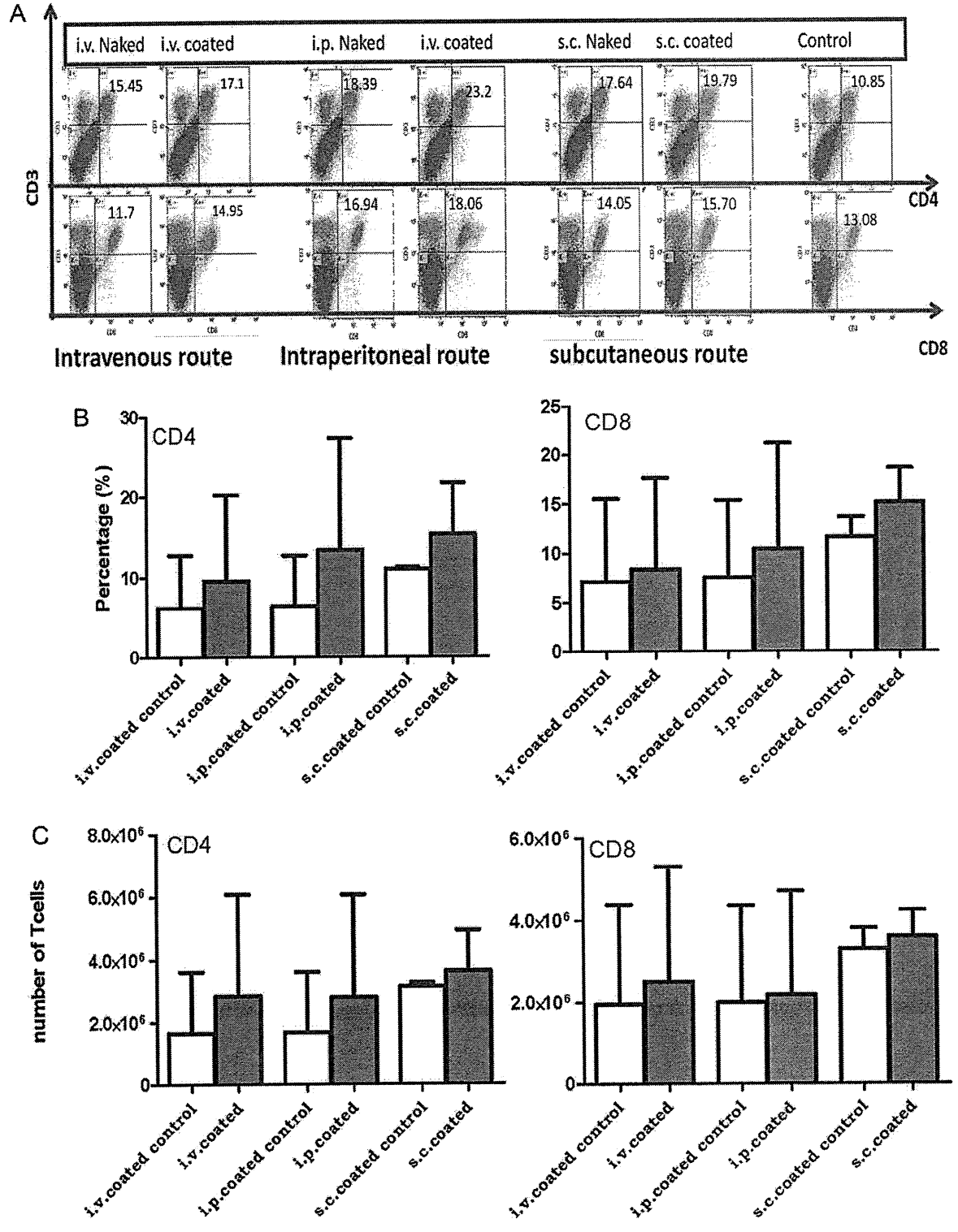

Fig. 3. Flow cytometric analysis of $CD4^+$ and $CD8^+$ T cell subpopulation. Mice were immunized either with nanoparticle coated or naked MSP-1 C-terminus plasmid or PBS. Two weeks after the last immunization, 2 mice from each group were sacrificed, their spleens removed and splenocytes were labeled with CD3-APC, CD4-FITC and CD8-PE cell surface markers.(A) Representative figure of proportion $CD4^+/CD3^+$ (green) $CD8^+/CD3^+$ (orange) from first experiment. (B and C) Stimulatory effect of coating on $CD4^+$ and $CD8^+$ T cell subpopulation in the spleen from second experiment. Mice were immunized either with NP-coated DNA or -coated blank plasmid. Two weeks after the last immunization, 2 mice from each group were sacrificed, their spleens removed and splenocytes were labeled with CD3-APC, CD4-FITC and CD8-PE cell surface markers and the T cell populations were determined by flow cytometry. Each bar representing mean ± SD taken from two different experiments. (C) Percentage of $CD4^+$ and $CD8^+$ T cells. (D) Absolute number of $CD4^+$ and $CD8^+$ T cells. (For interpretation of the references to color in this figure legend, the reader is referred to the web version of the article.)

to coated group in the previous experiments. In contrast, 50% of mice immunized sub-cutaneously with NP-coated plasmid survived from lethal *P. yoelii* challenge (Fig. 1B). To determine the antigen stimulatory effect of nanoparticle coating on antibody production, IgG and its subclass were measured in the serum collected 2 weeks after the last boost. Group of mice immunized by i.v. and i.p., with coated DNA plasmid showed high antibody titre as compared to the group of mice immunized with coated blank plasmid. However, no significant increase of antibody in the group of mice immunized s.c. route (Fig. 2A and D). Similar results were obtained using native crude antigen (Fig. S2). Flow cytometric analysis was performed on splenocytes by staining with surface molecules (CD3-APC, CD4-FITC and CD8-PE), and the percentage of $CD4^+$ and $CD8^+$ T cells was higher in the spleen of mice from the coated group as compared coated blank plasmid group across all the route administration (Fig. 3B). Furthermore, analysis of the absolute number of $CD4^+$ and $CD8^+$ T cells from the splenocyte of the mice vaccinated with coated DNA plasmid showed an increase across the three routes of administration (Fig. 3C).

3.2.1. On cytokine production

Four (4) cytokines (IL-4, IL-10, IL-12p40 and IFN-γ) were estimated from cultured splenocyte supernatants and pooled sera from each group of immunized mice. Significant differences were observed between the coated and coated-control groups from both the splenocyte cultured supernatants and pooled sera, across all the three routes of administration (Figs. 4A and B). IL-4 levels in mice immunized with coated vaccine by i.p. route, consistently showed significantly higher levels in both supernatant ($p = 0.02$) and serum ($p = 0.001$), respectively, as compared to coated blank plasmid immunized mice. Also IFN-γ ($p = 0.005$) and IL10 ($p = 0.001$) were significantly higher in the cultured splenocytes supernatant. Mice immunized with coated plasmid by s.c. route showed consistently significant elevation of IL-12p40 levels in both the serum and the supernatant ($p = 0.0006$ and $p = 0.01$, respectively) as compared to coated blank plasmid immunized mice. Analyses by Pearson rank test showed a positive correlation between protection and IL-12p40 cytokines levels in both serum ($r = 0.92$ and $p = 0.0083$) and supernatant ($r = 0.90$ and $p = 0.0065$) and IL-4 in the cultured splenocyte supernatant ($r = 0.84$ and $p = 0.018$). These results suggest that the most significant production of Th1 and Th2 cytokines from antigen reactive T cells were induced by i.p. followed by i.v. route of administration, while s.c. immunization activated only one of the Th1-type cytokines (IL-12p40).

3.2.2. On cytokine production of splenocytes stimulated with crude antigen (ELISPOT)

To evaluate the functional activity of splenocytes, ELISPOT assay was also performed to detect number of cells producing either IFN-γ or IL-4 in response to crude *P. yoelii* merozoite antigen. Number

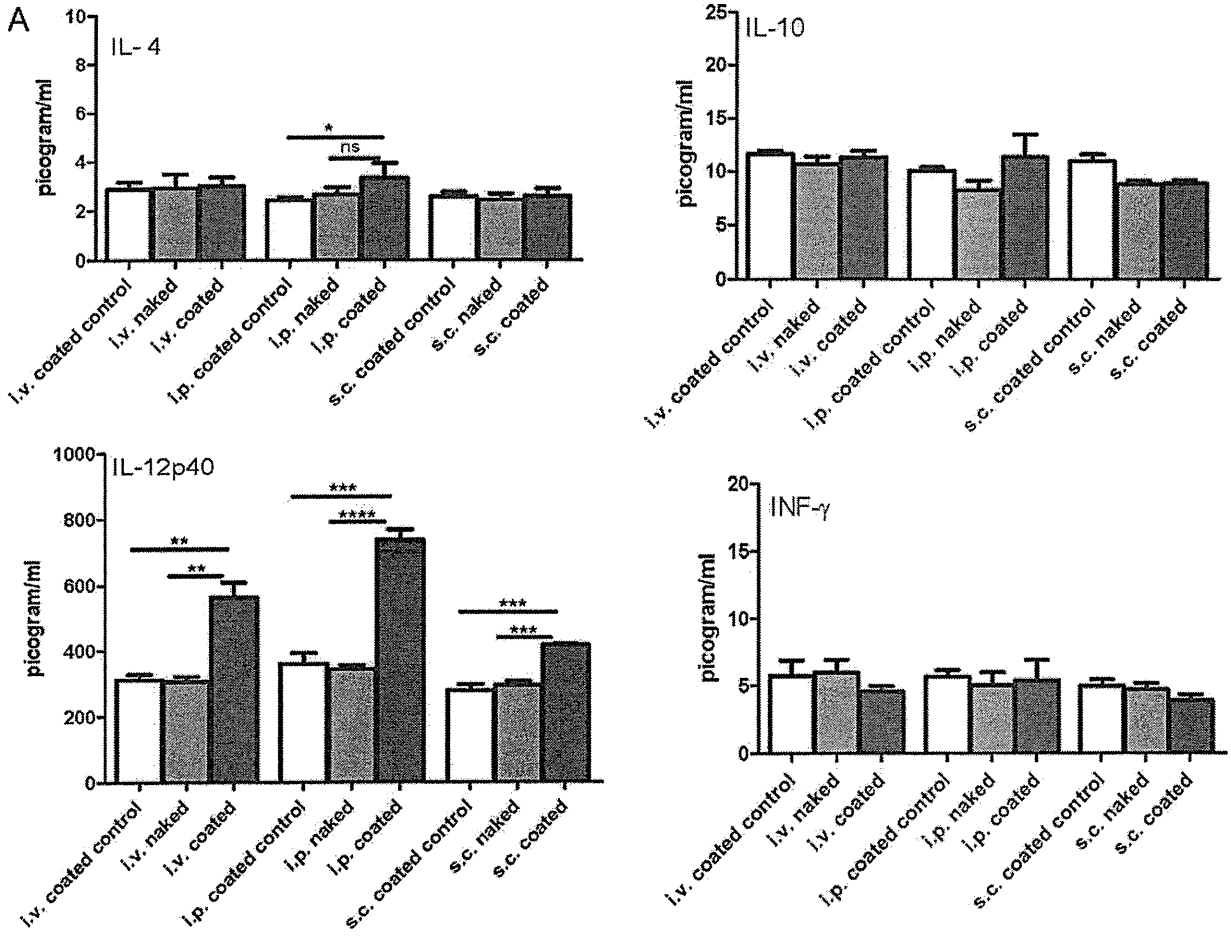

Fig. 4. Cytokine levels from pooled sera and cultured splenocytes supernatant from immunized mice from first and experiment. (A) Cytokine levels form pooled sera collected from mice in each group 2 weeks after the last immunization. (B) Cytokine levels in the splenocyte cultured supernatants: 2 weeks after the last immunization, 2 mice from each group were sacrificed, their spleens removed and splenocytes were prepared, cultured for 48 h and supernatant were collected. All cytokines were assayed using Procarta® Mouse Cytokine Plex kit. Each bar represents the mean ± SD of cytokine levels in quadruplicate wells. Comparison between coated and naked was done by student test. Statistical significance was designated as $p < 0.05$ (*$P \leq 0.05$; **$P \leq 0.01$; ***$P \leq 0.001$ and ****$P \leq 0.0001$).

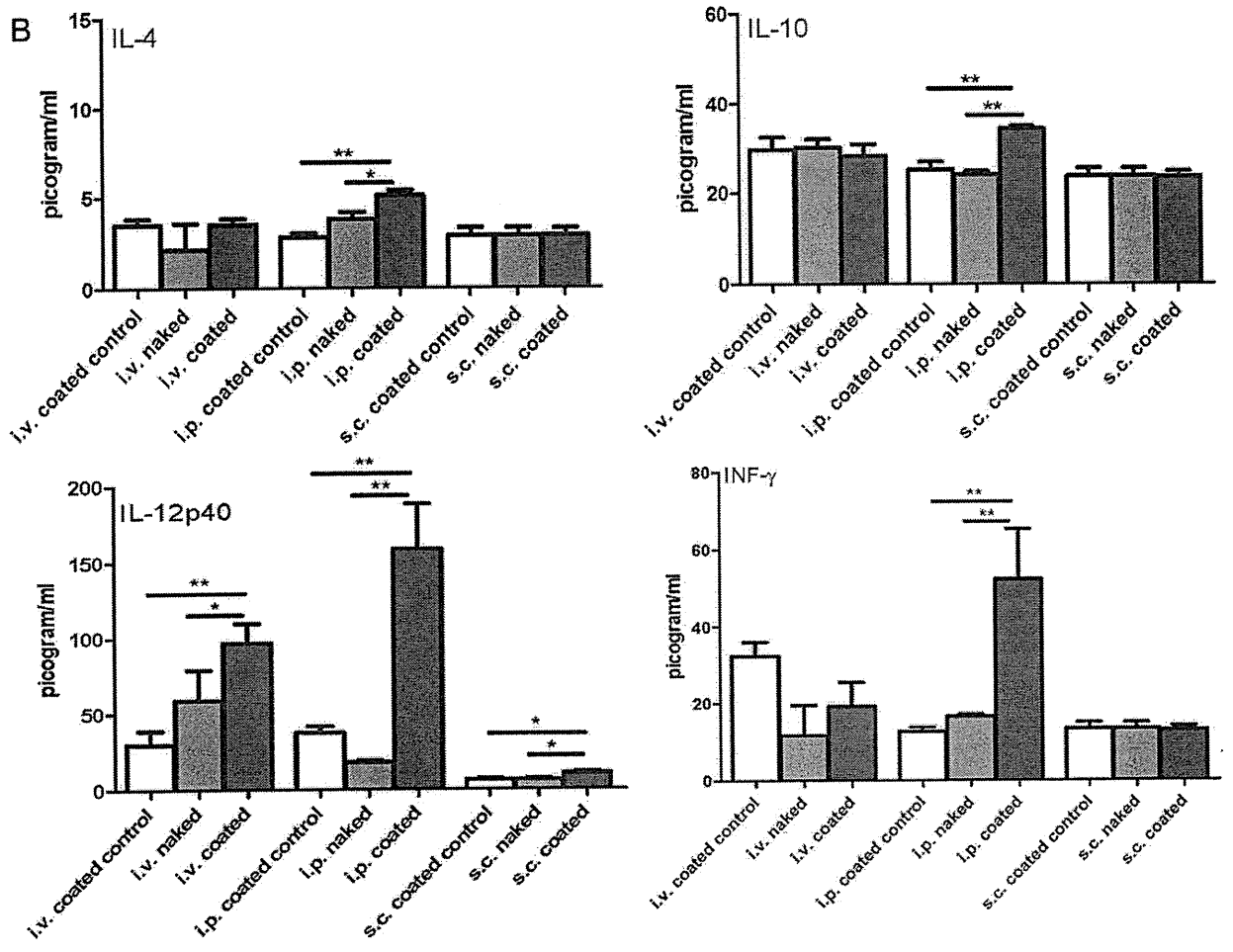

Fig. 4. *Continued.*

of IFN-γ-producing splenocytes in the coated group was more as compared to naked or control groups. However, the number IL-4-producing splenocytes was observed to be higher in the antigen stimulated coated group from coated-control groups (Fig. 5A and B). Pearson rank test showed a positive correlation between survival rate and INF-γ-producing splenocytes detected by ELISPOT assay ($r = 0.89$; $p = 0.0074$).

4. Discussion

DNA vaccines are yet to proceed beyond the phase two trials due to limited induction of desired immune response in humans. Efforts to identify methods of enhancing immune response of plasmid DNA vaccination have been tried [23,40–43] and among them is the development of delivery systems; which include delivery route and NP formulation [31,44,45]. Enhancing the immunogenicity of MSP-1; one of the leading malaria blood stage vaccine candidates [46], will be a very important step towards defeating malaria scourge. In this study, we have used two approaches (use of NP formulation and different routes of administration) to evaluate immunogenicity of C-terminus fragment of MSP-1. We have demonstrated the ability of the nanoparticle formulation used in this current study to enhance the immune response against *P. yoelii* lethal challenge across different routes of administration. It was observed that group of mice immunized with naked plasmid, developed high parasitaemia and was not able to control the parasite growth, and eventually died as compared to those mice immunized with NP-coated plasmid DNA in two different experiments.

Blood-stage malaria vaccine development is aimed at inducing high-titre growth-inhibitory antibodies against merozoite antigens involved in erythrocyte invasion [12,46]. High levels of protection against blood stage malaria were observed with elevated levels of IgG1 and IgG2a [47,48] and partial protection was observed when IgG1 and IgG2b predominates [30,47,49]. Here, the NP formulation enhanced the generation of antibody levels in the NP-coated plasmid DNA group. It was clearly shown that mice immunized with the NP-coated DNA plasmid produced high levels of IgG and its subtype antibodies (Fig. 2A–C). A significant difference of IgG subtypes (IgG2a and IgG2b) between NP-coated and naked plasmid DNA group in mice immunized by i.p. and i.v. routes of administration was observed (Fig. 2B and C) and this correlated with protection as previously reported [30,50,51].

It was reported that antibodies are required to reduce parasitaemia and $CD4^+$ T cells are required to achieve complete protection, probably to provide T cell help for antibody production [17]. Our data showed that, percentage of $CD4^+$ and $CD8^+$ T cells was high in mice immunized with coated plasmid DNA than those immunized with naked, across all the three routes of administration (Fig. 3). This is consistent with the low parasitaemia observed in mice from the coated group. We observed that survival rate in the group of immunized mice were strongly correlated (Pearson rank test) with IgG ($r = 0.62$; $p = 0.03$), IgG1 ($r = 0.59$; $p = 0.04$), IgG2a ($r = 0.7$; $p = 0.006$), and IgG2b ($r = 0.71$; $p = 0.01$) antibodies

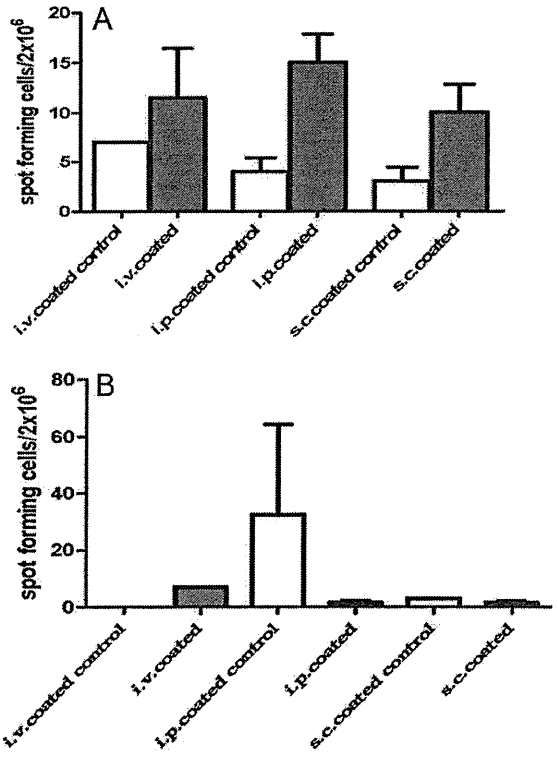

Fig. 5. Stimulatory effect of nanoparticle coating on antigen specific IL-4 and IFN-γ producing T cells in spleen as determined by ELISPOT. Splenocytes were prepared and cultured with *P. yoelii* crude antigen. Spot number evaluation was done automatically using an immunospot-image analyzer. 2×10^6 splenocyte/well were incubated 48 h in vitro with *P. yoelii* antigen or medium. (A) IFN-γ producing T cells, (B) IL-4 producing T cells in spleen. Each bar represents mean ± SD of spots number in duplicate wells.

estimated by ELISA. On the other hand, low antibody response in s.c. vaccinated mice, may explain the partial protection observed, although the T cells proportion in this group appeared to be higher than both the i.p. and i.v. vaccinated groups (Fig. 3). It was reported that antibodies are required to reduce parasitaemia in the first 12 days after challenge, and $CD4^+$ T cells are required to achieve complete protection [17], probably to provide T cell help for antibody production. It is interesting that the mice immunized with coated DNA plasmid by s.c. delivery route in the second experiment did not show elevated levels of anti-MSP-1 IgG and subtypes but exhibited 50% survival (Fig. 1A) and the survived mice developed high parasitaemia during the first 2 weeks post-infection although some were able to clear their parasitaemia afterwards (Fig. 1A).

Various studies have shown that, with the same formulation, route of injection influenced the immune response [35,52,53]. In the larger number of studies that have evaluated DNA-based immunization, few have directly compared the immune responses generated by different routes of delivery. Effective translation of this approach to human clinical setting could be tasking and perhaps controversial, particularly by IP route. IP vaccination is predominantly used in veterinary medicine due to the ease of administration compared with other parenteral methods and induction of protective immune response in several type of animals such as fish [54] chicken [55] and pigs [56,57]. Also, Lue et al. [58] reported that Ip vaccination of human subjects with tetanus toxoid induces specific immune response. Thus, we assumed that this formulation may work as well in mucosal route of delivery system, because it was reported that the peritoneal cavity contains a major reservoir of self-replenishing cells that play a significant role in the mucosal immune response [59,60]. Currently, modification to this formulation to fit into clinical setting is ongoing. Eventually, this would be feasible if the *Plasmodium falciparum* counterpart of MSP-1 is used and all the immunological parameters rival or better than the reported ones. However, in human IV routes are used to administer drugs [61] and vaccine [58].

It is believed that clearance of blood stage infection required Th1 and Th2 types of immune response. The observed complete protection against lethal challenge in immunized mice in the coated group of i.v. and i.p. routes of delivery may be partly explained by the contributory effect of IL-12p40, which may have induced a Th1 immune response. This effect is observable in s.c.-vaccinated group with low antibody production but with partial protection. It was reported that, IL-12p40 appears to be critically linked to or to act through IFN-γ production, thereby allowing an early and sustained Th1 response and is shown to be required for the production of protective IgG2a antibody [33,62–64]. However, a number of observations indicate that exposure to IL-4 is essential for the priming of Th2-type effector T cells [65]. These results suggest that enhanced Th1 and Th2 cytokines were induced by i.p. followed by i.v. route of administration, while marginally by s.c. immunization.

Nanoparticles are considered efficient immune–potentitor and antigen–carrier to DC [66,67] and γ-PGA nanoparticle induced DC activation by acting as a potent vaccine adjuvant as well as an efficient antigen carrier to DC [68]. This NP-coated MSP-1 formulation predominantly was taken up by DC and which started to produce IL-12 abundantly, essential for the priming of Th1-type effector T cells. Also, our data showed that NP coating is a promising strategy for potent induction of antigen specific immune responses. We have already reported the enhancing effect of nanoparticle coating for the MSP-1 DNA vaccination model, however, the level of protection and antibody production were not so higher as the current study [30]. One of the possible reasons might be the use of different vector named VR1020 that had been approved by FDA for human vaccine use. The major advantage of this vector is described elsewhere (Vical Incorporated, San Diego, CA).

In summary, vaccination with NP-coated MSP-1 C-terminus plasmid using three different routes of delivery was evaluated, and i.p. and i.v. delivery routes showed complete protection against lethal challenge with significant increase in levels of IgG and its subtypes and also of both Th1 and Th2 type cytokines production. On the other hand, in s.c. vaccinated group, mice showed about 50% protection and marginal levels of specific antibody. These findings, therefore, underscore the relevance of DNA vaccination and could be contributory to the current approaches to meet our desired goal of defeating malaria and other infection diseases.

Acknowledgements

We would like to thank Dr Shibata, H. for technical assistance and Vical incorporated for providing the vector VR1020 (Vical, San Diego, CA, USA). MSC is a graduate student under the GCOE program.

Appendix A. Supplementary data

Supplementary data associated with this article can be found, in the online version, at doi:10.1016/j.vaccine.2011.09.031.

References

[1] Snow RW, Guerra CA, Noor AM, Myint HY, Hay SI. The global distribution of clinical episodes of *Plasmodium falciparum* malaria. Nature 2005;434(March (7030)):214–7.
[2] Abdullah S, Adazu K, Masanja H, Diallo D, Hodgson A, Ilboudo-Sanogo E, et al. Patterns of age-specific mortality in children in endemic areas of sub-Saharan Africa. Am J Trop Med Hyg 2007;77(December (Suppl. 6)):99–105.

[3] Carneiro I, Roca-Feltrer A, Griffin JT, Smith L, Tanner M, Schellenberg JA, et al. Age-patterns of malaria vary with severity, transmission intensity and seasonality in sub-Saharan Africa: a systematic review and pooled analysis. PloS One 2010;5(2):e8988.
[4] Nosten F, White NJ. Artemisinin-based combination treatment of falciparum malaria. Am J Trop Med Hyg 2007;77(December (Suppl. 6)):181–92.
[5] Lengeler C, Snow RW. From efficacy to effectiveness: insecticide-treated bed nets in Africa. Bull World Health Organ 1996;74(3):325–32.
[6] Jha P. Reliable mortality data: a powerful tool for public health. Natl Med J India 2001;14(May–June (3)):129–31.
[7] Hay SI, Guerra CA, Gething PW, Patil AP, Tatem AJ, Noor AM, et al. A world malaria map: *Plasmodium falciparum* endemicity in 2007. PLoS Med 2009;6(March (3)):e1000048.
[8] Anderson T. Mapping the spread of malaria drug resistance. PLoS Med 2009;6(April (4)):e1000054.
[9] Hu J, Chen Z, Gu J, Wan M, Shen Q, Kieny MP, et al. Safety and immunogenicity of a malaria vaccine, *Plasmodium falciparum* AMA-1/MSP-1 chimeric protein formulated in montanide ISA 720 in healthy adults. PLoS One 2008;3(4):e1952.
[10] Nyarango PM, Gebremeskel T, Mebrahtu G, Mufunda J, Abdulmumini U, Ogbamariam A, et al. A steep decline of malaria morbidity and mortality trends in Eritrea between 2000 and 2004: the effect of combination of control methods. Malaria J 2006;5:33.
[11] Feachem R, Sabot O. A new global malaria eradication strategy. Lancet 2008;371(May (9624)):1633–5.
[12] Kang Y, Calvo PA, Daly TM, Long CA. Comparison of humoral immune responses elicited by DNA and protein vaccines based on merozoite surface protein-1 from *Plasmodium yoelii*, a rodent malaria parasite. J Immunol 1998;161(October (8)):4211–9.
[13] Boyle MJ, Wilson DW, Richards JS, Riglar DT, Tetteh KK, Conway DJ, et al. Isolation of viable *Plasmodium falciparum* merozoites to define erythrocyte invasion events and advance vaccine and drug development. Proc Natl Acad Sci USA 2010;107(August (32)):14378–83.
[14] Zhang Q, Xue X, Qu L, Pan W. Construction and evaluation of a multistage combination vaccine against malaria. Vaccine 2007;25(March (11)):2112–9.
[15] Good MF. Towards a blood-stage vaccine for malaria: are we following all the leads? Nat Rev Immunol 2001;1(November (2)):117–25.
[16] Greenwood B, Targett G. Do we still need a malaria vaccine? Parasite Immunol 2009;31(September (9)):582–6.
[17] Daly TM, Long CA. Humoral response to a carboxyl-terminal region of the merozoite surface protein-1 plays a predominant role in controlling blood-stage infection in rodent malaria. J Immunol 1995;155(July (1)):236–43.
[18] Hirunpetcharat C, Tian JH, Kaslow DC, van Rooijen N, Kumar S, Berzofsky JA, et al. Complete protective immunity induced in mice by immunization with the 19-kilodalton carboxyl-terminal fragment of the merozoite surface protein-1 (MSP1[19]) of *Plasmodium yoelii* expressed in *Saccharomyces cerevisiae*: correlation of protection with antigen-specific antibody titer, but not with effector $CD4^+$ T cells. J Immunol 1997;159(October (7)):3400–11.
[19] Blackman MJ, Heidrich HG, Donachie S, McBride JS, Holder AA. A single fragment of a malaria merozoite surface protein remains on the parasite during red cell invasion and is the target of invasion-inhibiting antibodies. J Exp Med 1990;172(July (1)):379–82.
[20] Wipasa J, Xu H, Liu X, Hirunpetcharat C, Stowers A, Good MF. Effect of *Plasmodium yoelii* exposure on vaccination with the 19-kilodalton carboxyl terminus of merozoite surface protein 1 and vice versa and implications for the application of a human malaria vaccine. Infect Immun 2009;77(February (2)):817–24.
[21] Okitsu SL, Silvie O, Westerfeld N, Curcic M, Kammer AR, Mueller MS, et al. A virosomal malaria peptide vaccine elicits a long-lasting sporozoite-inhibitory antibody response in a phase 1a clinical trial. PLoS One 2007;2(12):e1278.
[22] Moorthy VS, Good MF, Hill AV. Malaria vaccine developments. Lancet 2004;363(January (9403)):150–6.
[23] Gurunathan S, Klinman DM, Seder RA. DNA vaccines: immunology, application, and optimization*. Annu Rev Immunol 2000;18:927–74.
[24] ten Hagen TL, Sulzer AJ, Kidd MR, Lal AA, Hunter RL. Role of adjuvants in the modulation of antibody isotype, specificity, and induction of protection by whole blood-stage *Plasmodium yoelii* vaccines. J Immunol 1993;151(December (12)):7077–85.
[25] Malyala P, Singh M. Micro/nanoparticle adjuvants: preparation and formulation with antigens. Methods Mol Biol 2010;626:91–101.
[26] van Zanten J, Doornbos-Van der Meer B, Audouy S, Kok RJ, de Leij L. A non-viral carrier for targeted gene delivery to tumor cells. Cancer Gene Ther 2004;11(February (2)):156–64.
[27] Peek LJ, Middaugh CR, Berkland C. Nanotechnology in vaccine delivery. Adv Drug Deliv Rev 2008;60(May (8)):915–28.
[28] Kaba SA, Brando C, Guo Q, Mittelholzer C, Raman S, Tropel D, et al. A non-adjuvanted polypeptide nanoparticle vaccine confers long-lasting protection against rodent malaria. J Immunol 2009;183(December (11)):7268–77.
[29] Kurosaki T, Kitahara T, Fumoto S, Nishida K, Nakamura J, Niidome T, et al. Ternary complexes of pDNA, polyethylenimine, and gamma-polyglutamic acid for gene delivery systems. Biomaterials 2009;30(May (14)):2846–53.
[30] Shuaibu MN, Cherif MS, Kurosaki T, Helegbe GK, Kikuchi M, Yanagi T, et al. Effect of nanoparticle coating on the immunogenicity of plasmid DNA vaccine encoding *P. yoelii* MSP-1 C-terminal. Vaccine 2011;29(April (17)):3239–47.
[31] Bohm W, Mertens T, Schirmbeck R, Reimann J. Routes of plasmid DNA vaccination that prime murine humoral and cellular immune responses. Vaccine 1998;16(May–June (9–10)):949–54.
[32] Johansson EL, Bergquist C, Edebo A, Johansson C, Svennerholm AM. Comparison of different routes of vaccination for eliciting antibody responses in the human stomach. Vaccine 2004;22(February (8)):984–90.
[33] Su Z, Stevenson MM. IL-12 is required for antibody-mediated protective immunity against blood-stage Plasmodium chabaudi AS malaria infection in mice. J Immunol 2002;168(February (3)):1348–55.
[34] Lodmell DL, Ray NB, Ulrich JT, Ewalt LC. DNA vaccination of mice against rabies virus: effects of the route of vaccination and the adjuvant monophosphoryl lipid A (MPL). Vaccine 2000;18(January (11–12)):1059–66.
[35] Tang DC, DeVit M, Johnston SA. Genetic immunization is a simple method for eliciting an immune response. Nature 1992;356(March (6365)):152–4.
[36] McCluskie MJ, Brazolot Millan CL, Gramzinski RA, Robinson HL, Santoro JC, Fuller JT, et al. Route and method of delivery of DNA vaccine influence immune responses in mice and non-human primates. Mol Med 1999;5(May (5)):287–300.
[37] Aguiar JC, Hedstrom RC, Rogers WO, Charoenvit Y, Sacci Jr JB, Lanar DE, et al. Enhancement of the immune response in rabbits to a malaria DNA vaccine by immunization with a needle-free jet device. Vaccine 2001;20(October (1–2)):275–80.
[38] Tsuboi T, Takeo S, Iriko H, Jin L, Tsuchimochi M, Matsuda S, et al. Wheat germ cell-free system-based production of malaria proteins for discovery of novel vaccine candidates. Infect Immun 2008;76(April (4)):1702–8.
[39] Tsuboi T, Takeo S, Sawasaki T, Torii M, Endo Y. An efficient approach to the production of vaccines against the malaria parasite. Methods Mol Biol 2010;607:73–83.
[40] Wang R, Epstein J, Baraceros FM, Gorak EJ, Charoenvit Y, Carucci DJ, et al. Induction of CD4(+) T cell-dependent CD8(+) type 1 responses in humans by a malaria DNA vaccine. Proc Natl Acad Sci USA 2001;98(September (19)):10817–22.
[41] Epstein JE, Gorak EJ, Charoenvit Y, Wang R, Freydberg N, Osinowo O, et al. Safety, tolerability, and lack of antibody responses after administration of a PfCSP DNA malaria vaccine via needle or needle-free jet injection, and comparison of intramuscular and combination intramuscular/intradermal routes. Hum Gene Ther 2002;13(September (13)):1551–60.
[42] Epstein JE, Charoenvit Y, Kester KE, Wang R, Newcomer R, Fitzpatrick S, et al. Safety, tolerability, and antibody responses in humans after sequential immunization with a PfCSP DNA vaccine followed by the recombinant protein vaccine RTS,S/AS02A. Vaccine 2004;22(April (13–14)):1592–603.
[43] Dobano C, Sedegah M, Rogers WO, Kumar S, Zheng H, Hoffman SL, et al. Plasmodium: mammalian codon optimization of malaria plasmid DNA vaccines enhances antibody responses but not T cell responses nor protective immunity. Exp Parasitol 2009;122(June (2)):112–23.
[44] Yokoyama M, Zhang J, Whitton JL. DNA immunization: effects of vehicle and route of administration on the induction of protective antiviral immunity. FEMS Immunol Med Microbiol 1996;14(July (4)):221–30.
[45] Barry MA, Johnston SA. Biological features of genetic immunization. Vaccine 1997;15(June (8)):788–91.
[46] Holder AA. The carboxy-terminus of merozoite surface protein 1: structure, specific antibodies and immunity to malaria. Parasitology 2009;136(October (12)):1445–56.
[47] Ling IT, Ogun SA, Momin P, Richards RL, Garcon N, Cohen J, et al. Immunization against the murine malaria parasite *Plasmodium yoelii* using a recombinant protein with adjuvants developed for clinical use. Vaccine 1997;15(October (14)):1562–7.
[48] De Souza JB, Ling IT, Ogun SA, Holder AA, Playfair JH. Cytokines and antibody subclass associated with protective immunity against blood-stage malaria in mice vaccinated with the C terminus of merozoite surface protein 1 plus a novel adjuvant. Infect Immun 1996;64(September (9)):3532–6.
[49] Tongren JE, Corran PH, Jarra W, Langhorne J, Riley EM. Epitope-specific regulation of immunoglobulin class switching in mice immunized with malarial merozoite surface proteins. Infect Immun 2005;73(December (12)):8119–29.
[50] Diallo TO, Spiegel A, Diouf A, Perraut R, Kaslow DC, Garraud O. Short report: IgG1/IgG3 antibody responses to various analogs of recombinant ypfmsp119—a study in immune adults living in areas of *Plasmodium falciparum* transmission. Am J Trop Med Hyg 2001;64(March–April (3–4)):204–6.
[51] Garraud O, Mahanty S, Perraut R. Malaria-specific antibody subclasses in immune individuals: a key source of information for vaccine design. Trends Immunol 2003;24(January (1)):30–5.
[52] Boyle JS, Silva A, Brady JL, Lew AM. DNA immunization: induction of higher avidity antibody and effect of route on T cell cytotoxicity. Proc Natl Acad Sci USA 1997;94(December (26)):14626–31.
[53] Playfair JH, De Souza JB. Vaccination of mice against malaria with soluble antigens. I. The effect of detergent, route of injection, and adjuvant. Parasite Immunol 1986;8(September (5)):409–14.
[54] Caipang CM, Hynes N, Puangkaew J, Brinchmann MF, Kiron V. Intraperitoneal vaccination of Atlantic cod, *Gadus morhua* with heat-killed *Listonella anguillarum* enhances serum antibacterial activity and expression of immune response genes. Fish Shellfish Immunol 2008;24(March (3)):314–22.
[55] Muir WI, Bryden WL, Husband AJ. Evaluation of the efficacy of intraperitoneal immunization in reducing *Salmonella typhimurium* infection in chickens. Poult Sci 1998;77(December (12)):1874–83.
[56] Sheldrake RF, Romalis LF, Saunders MM. Serum mucosal antibody responses against *Mycoplasma hyopneumoniae* following intraperitoneal vaccination and challenge of pigs with *M. hyopneumoniae*. Res Vet Sci 1993;55(November (3)):371–6.